Calculation of lepton magnetic moments in quantum electrodynamics: A justification of the flexible divergence elimination method

Sergey Volkov●[*]

Institute for Theoretical Physics, Karlsruhe Institute of Technology (KIT), 76128 Karlsruhe, Germany

The flexible method of reduction to finite integrals, briefly described in earlier publications of the author, is described in detail. The method is suitable for the calculation of all quantum electrodynamical contributions to the magnetic moments of leptons. It includes mass-dependent contributions. The method removes all divergences (UV, IR, and mixed) point-by-point in Feynman parametric space without any usage of limitlike regularizations. It yields a finite integral for each individual Feynman graph. The subtraction procedure is based on the use of linear operators applied to the Feynman amplitudes of UV-divergent subgraphs; a placement of all terms in the same Feynman parametric space is implied. The final result is simply the sum of the individual graph contributions; no residual renormalization is required. The method also allows us to split the total contribution into the contributions of small gauge-invariant classes. The procedure offers a great freedom in the choice of the linear operators. This freedom can be used for improving the computation speed and for a reliability check. The mechanism of divergence elimination is explained, as well as the equivalence of the method and the on shell renormalization. For illustrative purposes, all 4-loop contributions to the anomalous magnetic moments of the electron and muon are given for each small gauge-invariant class, as well as their comparison with previously known results. This also includes the contributions that depend on the ratios of the tau-lepton mass to the electron and muon mass.

I. INTRODUCTION

A. Quantum field theory, divergences, and renormalization

It is well known that the first formulations of quantum field theory suffered from ultraviolet (UV) divergences. In 1947–1949, the first results appeared showing that the UV divergences in the physical observables are canceled if we define the physical parameters properly. This demonstration was the result of the efforts of R. Feynman, J. Schwinger, H. Bethe, S. Tomonaga, and others. A procedure for dealing with UV divergences in quantum electrodynamics (QED) at any order of the perturbation series was developed by F. J. Dyson [1] and A. Salam [2]. A further development and a mathematical understanding of these ideas has led to N. Bogoliubov's $\mathcal{R}$-operation. This operation can be represented as a subtraction procedure that deals with the Feynman amplitudes of the UV-divergent subgraphs in each Feynman graph that contributes to the needed probability

amplitude; it removes all UV divergences in each Feynman graph. The application of the $\mathcal{R}$-operation to Feynman graphs is equivalent to an introduction of counterterms into the Lagrangian; it can be treated as a renormalization of the theory parameters. The corresponding theorem was proved in 1956 by N. Bogoliubov and O. Parasiuk [3]. This proof contains some inaccuracies, but nevertheless, the Bogoliubov-Parasiuk theorem set a standard of quality and raised the hope that quantum field theory has a meaning and can be rigorously examined. The shortcomings of the proof were corrected by K. Hepp in 1964 [4].

Not only the Bogoliubov-Parasiuk-Hepp theorem is of interest, but also its proof, because a stronger statement was proved: the UV subtractions lead directly to finite integrals in Schwinger parametric space.[1] In QED, we have Feynman graphs with the propagators,

---

[*]sergey.volkov.1811@gmail.com, volkoff˙sergey@mail.ru, sergey.volkov@partner.kit.edu

---

[1]Usually, these statements are referred to as the BPHZ approach. The last letter "Z" refers to W. Zimmermann's paper [5]. In that work, the convergence theorem was proved directly in Minkowsky momentum space. Moreover, an explicit solution of the recurrence relations given by the $\mathcal{R}$-operation was provided, also known as Zimmermann's forest formula (more precisely, the solution had been provided four years earlier by O. I. Zavialov and B. M. Stepanov [6], but this publication was only in Russian and was not noticed).

$$\frac{i(\not{q}+m)}{q^2-m^2+i\varepsilon}, \qquad \frac{-g_{\mu\nu}}{q^2+i\varepsilon}, \tag{1}$$

for the lepton and photon lines correspondingly, where $\not{q}=q^\nu\gamma_\nu$ stands for the Dirac gamma matrices γ_ν. If we transfer to the Schwinger parameters by using the formula,

$$\frac{i}{x}=\int_0^{+\infty}e^{ixz}dz,$$

we express the Feynman amplitude as an integral,

$$\int_{z_1,\dots,z_L>0} I(z_1,\dots,z_L,p_1,\dots,p_n,\varepsilon)dz_1\dots dz_L, \tag{2}$$

where $p=(p_1,\dots,p_n)$ is the vector of external momenta, $z=(z_1,\dots,z_L)$ is the vector of Schwinger parameters, z_j corresponds to the jth internal line of the graph. If we apply the $\mathcal{R}$-operation, $I(z_1,\dots,z_L,p_1,\dots,p_n,\varepsilon)$ is expressed as a linear combination of terms; each term is a product of some functions, each of which corresponds to a Feynman amplitude that uses a subset of the set of internal lines; if the same mapping is used between z_j and the internal lines, all the counterterms are placed in the same Schwinger parametric space. A by-product of the Bogoliubov-Parasiuk-Hepp theorem is that (2) is finite for any $\varepsilon>0$.

Unfortunately, these subtractions in Schwinger's parametric space are useless for calculations. The reason is the inability to handle the limit $\varepsilon\to 0$. Infrared (IR) divergences and their cancellation have been widely discussed in literature. However, a rigorous examination for the general case has not yet been done. At higher orders IR and UV divergences mix with each other.[2] In the case of magnetic moments of leptons, all IR divergences are removed by the physical on shell renormalization as well as the UV and mixed ones.[3] A general scattering process requires consideration of a finite photon detector sensitivity in addition to renormalization. The on shell renormalization can be performed in place in Feynman graphs by a simple modification of the $\mathcal{R}$-operation. In the case of the lepton magnetic moments, it removes all divergences in the final result. However, the individual integrals remain IR divergent.

The combinatorics of the IR and mixed divergences in Feynman graphs is very complicated. For this reason, their subtraction before integration is very rarely used in modern quantum field theory computations. Nowadays, most calculations use dimensional regularization, which allows us to work directly with infinite components without exact mappings for cancellation. However, the use of dimensional regularization requires an enormous amount of symbolic manipulation at higher orders. An experience

with calculations of the lepton magnetic moment shows that the methods that subtract divergences before integration work much faster and allow us to obtain high-order corrections that are not achievable with other methods.

B. Anomalous magnetic moments of leptons and their calculations

The anomalous magnetic moments (AMM) of the electron and muon are known with a very high precision. A recent measurement [10] gave the result,

$$a_e=0.00115965218059(13). \tag{3}$$

Standard Model predictions for the electron AMM a_e use the following expression:

$$a_e=a_e(\text{QED})+a_e(\text{hadronic})+a_e(\text{electroweak}),$$

$$a_e(\text{QED})=\sum_{n\geq 1}\left(\frac{\alpha}{\pi}\right)^n a_e^{2n},$$

$$a_e^{2n}=A_1^{(2n)}+A_2^{(2n)}(m_e/m_\mu)+A_2^{(2n)}(m_e/m_\tau)$$
$$+A_3^{(2n)}(m_e/m_\mu,m_e/m_\tau),$$

where m_e,m_μ,m_τ are the masses of the electron, muon, and tau-lepton, respectively, α is the fine-structure constant; a similar expression is used for the muon AMM a_μ.

The universal QED terms $A_1^{(2n)}(\alpha/\pi)^n$ form the main contribution to a_e and a_μ. The value,

$$A_1^{(2)}=0.5,$$

was obtained in 1948 by J. Schwinger [11,12]. The 2-loop contribution $A_1^{(4)}$ was calculated mainly by R. Karplus and N. Kroll [13]. However, this calculation had an error; the correct value,

$$A_1^{(4)}=-0.328478965579\dots,$$

was independently presented by A. Petermann [14] and C. Sommerfeld [15] in 1957. The value of $A_1^{(6)}$ was being calculated in 1970-x by various research groups using numerical integration ([16,17]; [18]; [19]). Each of these groups used its own method of divergence elimination at the integrand level. The most accurate value $A_1^{(6)}=1.195\pm 0.026$ for those times was obtained in 1974 by T. Kinoshita and P. Cvitanović; the uncertainty is caused by the statistical error of the Monte Carlo integration. At the same time, an analytical calculation of $A_1^{(6)}$ using computers was started. The final value,

$$A_1^{(6)}=1.181241456\dots,$$

---

[2]See, e.g., the explicit formulas in [7].
[3]See, for example, [8] and Appendix C of [9].

was obtained by S. Laporta and E. Remiddi in 1996 [20]. This value was the result of the efforts of many researchers (see, for example, [21–26]). First numerical estimates for $A_1^{(8)}$ were obtained by T. Kinoshita and W. B. Lindquist in 1981 [27]. The most accurate value presented by T. Kinoshita's team, $A_1^{(8)} = -1.91298(84)$, was published in 2015 [28]. This value was obtained by Monte Carlo integration. The semianalytic result of S. Laporta,

$$A_1^{(8)} = -1.9122457649\ldots,$$

was obtained in 2017 [29]. These two calculations of $A_1^{(8)}$ agree well, as do another independent calculations [30,31] and our calculation of Feynman graphs without lepton loops [32]. First overall calculation results for $A_1^{(10)}$ were published in 2012 by Aoyama-Hayakawa-Kinoshita-Nio (AHKN) in [33].[4] The last value obtained by this group in 2019 [34] is

$$A_1^{(10)}[\text{AHKN}] = 6.737(159). \qquad (4)$$

This coefficient has not yet been verified, and a significant computational error could be apparent in experiments. We recalculated the total contribution of the graphs without lepton loops to $A_1^{(10)}$ and presented [35] in 2019 the value,

$$A_1^{(10)}[\text{no lepton loops, Volkov}] = 6.793(90),$$

that leads to

$$A_1^{(10)}[\text{Volkov} + \text{AHKN}] = 5.862(90), \qquad (5)$$

with a discrepancy of 4.8σ with (4). At the moment the discrepancy is unresolved, but independent calculations are coming [36]. The values (4) and (5) in combination with the experimental value (3) and another known contribution [34] lead to

$$\alpha^{-1}[a_e, \text{AHKN}] = 137.0359991663(155) \qquad (6)$$

and

$$\alpha^{-1}[a_e, \text{Volkov} + \text{AHKN}] = 137.0359991593(155), \qquad (7)$$

correspondingly. The values obtained from the measured ratios of the atomic masses and the Planck constant,

---

[4]And another subtraction procedure that removes all divergences before integration was developed for these calculations; it is different from those used for sixth and eighth order calculations.

$$\alpha^{-1}[\text{Rb} - 2011] = 137.035998996(85),$$
$$\alpha^{-1}[\text{Cs} - 2018] = 137.035999046(27),$$
$$\alpha^{-1}[\text{Rb} - 2020] = 137.035999206(11),$$

come from [37,38,39], respectively. Note that $\alpha^{-1}[\text{Rb} - 2020]$ is the largest among these three values and has a discrepancy of 5.4σ relative to $\alpha^{-1}[\text{Cs} - 2018]$. The tensions with (6) are 1.97σ, 3.86σ, 2.09σ; the corresponding tensions with (7) are 1.89σ, 3.64σ, 2.46σ.

Other results exist for small classes of 5-loop and higher order graphs [40–42]; they are in good agreement with the ones mentioned above.

An analytic formula for $A_2^{(4)}(x)$ was first established by H. H. Elend [43] in 1966. Numerical values for $A_2^{(6)}$ appeared about 1969 [44]. Most attention was paid to $A_2^{(6)}(m_\mu/m_e)$, because its value $A_2^{(6)}(m_\mu/m_e) \approx 20$ became unexpectedly large. These values were also being calculated analytically in the form of an expansion in the mass ratio. These expansions are being published since 1975 with an increasing number of terms [45–49]. The values $A_3^{(6)}$ were also evaluated numerically [50], semianalytically [46], and analytically [51] as expansions in the mass ratios. First, numerical values of $A_2^{(8)}(m_\mu/m_e)$ appeared in 1990 [50]. The recent values of $A_2^{(8)}$ and $A_3^{(8)}$ for the electron and muon obtained by T. Aoyama and co-workers with the help of Monte Carlo integration are presented in [28,52]. Semianalytic calculations using expansions in mass ratios confirmed these results [53,54]. Other results for certain classes of graphs are also in good agreement with them [55–61]. The only known values of $A_2^{(10)}$ and $A_3^{(10)}$ for the electron and muon were presented in 2012 by T. Aoyama and co-workers [33,52]. Partial calculations of small graph classes confirm these results [42,46,57,62]. However, a very important contributing to a_μ value,

$$A_2^{(10)}(m_\mu/m_e) = 742.18(87),$$

has not been double-checked yet. It is much larger (in absolute value) than the corresponding electron value. A significant error in this value could be noticeable in experiments, and the shift would be comparable to the hadronic uncertainty. In addition, rapid growth of $A_2^{(2n)}(m_\mu/m_e)$ with n may cause the higher-order terms to significantly affect the result. However, estimates based on known lower-order values and renormgroup-inspired arguments [50,52,63–65], as well as nonrelativistic calculations [66], show that both possibilities seem unlikely.

See reviews [67] on the muon (2021) and [34] on the electron (2019) for details.

C. Methods of numerical calculation and gauge-invariant classes

Methods based on subtraction of divergences before integration have been widely used for calculations of QED contributions to magnetic moments of leptons [16,18,19,34] and for other quantum field theory calculations [68].

In 2016, we presented a method [69] suitable for computing $A_1^{(2n)}$ for arbitrary n. The difference of this method from the previously known methods is that it is based on linear operators applied to the Feynman amplitudes of UV-divergent subgraphs, and the final result is obtained directly by summing the contributions of the Feynman graphs (no residual renormalization is required).

A distribution of the final result over Feynman graphs is a matter of free choice, but it is very untrivial to realize this freedom in the context of methods that subtract divergences before integration and yield the final result without residual renormalization, because the integrals obtained must be finite for each individual Feynman graph, but the whole procedure must conform to the physical on shell renormalization. In a sense, this subtraction procedure must contain an evidence that the on shell renormalization removes all divergences, including infrared and mixed divergences. In 2021, we presented a modification [70] of the developed method; it allows us to choose three linear subtraction operators independently.[5] Moreover, the new method is suitable for the calculation of mass-dependent contributions $A_2^{(2n)}$, $A_3^{(2n)}$.[6]

Some classes of Feynman graphs form gauge-invariant classes. For example, any class of graphs closed under a motion of the internal photon lines along the lepton paths and loops, but without jumping over the external photon line, is invariant in the class of Lorentz-invariant gauges with the photon propagators of the form $-(g_{\mu\nu} + k_\mu k_\nu f(k^2))/(k^2 + i0)$, if we properly define the on shell renormalization for subclasses of graphs,[7,8] see Sec. IV A.

Examples of the use of the new method, as well as a comparison with the old method, were given in [70,71]. In this work, we show that the method yields the exact value for each gauge-invariant class mentioned above, including those contributing to $A_2^{(2n)}$ and $A_3^{(2n)}$, as well as a finite integral for each Feynman graph.

II. THE METHOD FORMULATION

We work in the unit system where $\hbar = c = 1$, the factors of 4π appear in the fine-structure constant: $\alpha = e^2/(4\pi)$, the tensor $g_{\mu\nu}$ corresponds to the signature $(+, -, -, -)$, the Dirac matrices satisfy the condition $\gamma_\mu\gamma_\nu + \gamma_\nu\gamma_\mu = 2g_{\mu\nu}$. We also suppose $e = 1$ for the lepton electric charge; since we work with each term of the perturbation series separately, it changes nothing, but makes the expressions shorter.

We extract the lepton AMM from QED Feynman graphs with $N_l = 2$, $N_\gamma = 1$, where by N_l and N_γ we denote the number of external lepton and photon lines in the graph; each graph may contain electron, muon, tau-lepton lines. We also assume that all graphs are one-particle irreducible and have no odd lepton loops (Furry's theorem).

We work in the Feynman gauge with the propagators (1) for leptons and photons, respectively, where m is the lepton mass.

There are the following types of UV-divergent subgraphs[9] in QED Feynman graphs: *lepton self-energy* subgraphs ($N_l = 2$, $N_\gamma = 0$), *vertexlike* subgraphs ($N_l = 2$, $N_\gamma = 1$), *photon self-energy* subgraphs ($N_l = 0$, $N_\gamma = 2$), *photon-photon scattering* subgraphs[10] ($N_l = 0$, $N_\gamma = 4$).

Two subgraphs are said to overlap if they are not contained in each other and the intersection of their line sets is not empty.

A set of subgraphs of a graph is called a *forest* if any two elements of this set do not overlap.

For a vertexlike graph G, we denote by $\mathfrak{F}[G]$ the set of all forests F consisting of UV-divergent subgraphs of G and satisfying the condition $G \in F$. The lepton path of a graph G connecting its external lepton lines is called the *main path* of G. By $\mathcal{I}[G]$, we denote[11] the set of all vertexlike subgraphs of G (including G), which have the vertex incident to the external photon of G and at least one vertex of the main path of G.

To define the subtraction procedure, we use the linear operators labeled A, U_0, U_1, U_2, U_3, L; sometimes the same names are used for operators applied to the Feynman amplitudes of subgraphs of different types. The definitions are

---

[5]The number is not related to the number of leptons; the number of leptons can be arbitrarily large.

[6]More precisely, the old method is also suitable for this, but the argument in [69] does not prove this and is not extensible to prove this.

[7]The gauge invariance was proved in [8], but only for graphs without lepton loops. It looks the whole proof is not published, but the fact is widely used; we believe that the ideas of [8] can be extended to the general case.

[8]The gauge invariance implies not only the possibility of using different photon propagators, but also the ability to renormalize photon self-energies differently.

[9]We consider only those subgraphs, which are one-particle irreducible and contain all lines connecting the vertexes of the given subgraph; since odd lepton loops are forbidden, a UV-divergent subgraph is one-particle irreducible if and only if it is amputated.

[10]Photon-photon scattering subgraph divergences cancel in the final result without subtraction, but they remain in the individual graphs.

[11]The definition differs from that in [69].

(i) A is applied to vertexlike Feynman amplitudes[12] $\Gamma_\mu(p, q)$ and is defined as

$$(A\Gamma)_\mu(p, q) = [A'\Gamma]\gamma_\mu,$$

where A' is the projector of the AMM. See the definition of the projector in [35,69].

(ii) L is the standard on shell renormalization operator for vertexlike graphs; it is defined as

$$(L\Gamma)_\mu(p, q) = [L'\Gamma]\gamma_\mu,$$
$$L'\Gamma = a(m^2) + mb(m^2) + m^2 c(m^2),$$

where

$$\Gamma_\mu(p, 0) = a(p^2)\gamma_\mu + b(p^2)p_\mu + c(p^2)\not{p}p_\mu$$
$$+ d(p^2)(\not{p}\gamma_\mu - \gamma_\mu\not{p}). \quad (8)$$

(iii) U_0 is applied to photon self-energy and photon-photon scattering subgraphs and works as in standard renormalization. For the Feynman amplitude $\Pi_{\mu\nu}(p^2)$ of the photon self-energy, we can take, for example,

$$(U_0\Pi)_{\mu\nu}(p^2) = [U_0'\Pi][g_{\mu\nu}, p^2 g_{\mu\nu}, p_\mu p_\nu], \quad (9)$$

where

$$U_0'\Pi = \left[h_1(0), \frac{\partial h_1(p^2)}{\partial p^2}\bigg|_{p^2=0}, h_2(0) \right], \quad (10)$$

a scalar product is implied, and

$$\Pi_{\mu\nu}(p^2) = h_1(p^2)g_{\mu\nu} + h_2(p^2)p_\mu p_\nu. \quad (11)$$

Optimizations as described in [72] can also be used for photon self-energy graphs; the choice of the photon self-energy renormalization method does not play an important role in our subtraction procedure. For example, a more efficient method was used for the calculations; see Sec. V. However, the definition given here is convenient for proofs.

For the Feynman amplitudes of photon-photon scattering, we can take

$$(U_0\Pi)_{\mu_1\mu_2\mu_3\mu_4}(p_1, p_2, p_3, p_4) = \Pi_{\mu_1\mu_2\mu_3\mu_4}(0, 0, 0, 0),$$

where zero 4-momenta are denoted by 0. It also can be defined with vector-valued operators U_0' as it was done for photon self-energy Feynman amplitudes.

(iv) U_j, $j = 1$, 2 are applied to vertexlike and lepton self-energy Feynman amplitudes; U_3 is applied only to vertexlike amplitudes. They are defined as

$$(U_j\Gamma)_\mu(p, q) = [U_j'\Gamma]\gamma_\mu,$$

$$(U_j\Sigma)(p) = M'\Sigma + (U_j'\Sigma) \times (\not{p} - m), \quad (12)$$

where $\Gamma_\mu(p, q)$ and $\Sigma(p)$ are vertexlike and lepton self-energy Feynman amplitudes, U_j' are number-valued linear operators,

$$\Sigma(p) = r(p^2) + s(p^2)\not{p}. \quad (13)$$

$$M'\Sigma = r(m^2) + s(m^2)m. \quad (14)$$

We require that

(1) U_j ($j = 1$, 2) *preserve the Ward identity*: if Γ_μ and Σ satisfy

$$\Gamma_\mu(p, 0) = -\frac{\partial \Sigma(p)}{\partial p^\mu},$$

then

$$(U_j\Gamma)_\mu(p, 0) = -\frac{\partial[(U_j\Sigma)(p)]}{\partial p^\mu}$$

is also satisfied. The latter can be rewritten as

$$U_j'\Gamma = -U_j'\Sigma.$$

(2) If $\Gamma_\mu(p, 0) = 0$, then $U_j'\Gamma = 0$ ($j = 1$, 2, 3). We emphasize that the same symbol U_j is used for lepton self-energy and vertexlike Feynman amplitudes; the definitions for the different types are independent from each other, the requirements connect them.

These conditions are sufficient to prove combinatorially that the subtraction procedure defined below is equivalent to on shell renormalization, provided that all regularization issues are resolved.

To obtain finite integrals for each graph, more stringent requirements are needed. We take

$$U_j'\Gamma = a(M^2), \qquad U_j'\Sigma = -s(M^2), \qquad j = 1, 2,$$

where (8), (13) are satisfied, M^2 is an arbitrary real number (it may be different for different operators). As $U_3'\Gamma$ we can take $a(M^2)$ or $L'\Gamma$.

Being an operator means that it is applied to a function and depends only on this function (it does not depend on the internal structure of the corresponding subgraph). However, the same symbol U_j is used for linear operators that are applied to

---

[12]$p - \frac{q}{2}$, $p + \frac{q}{2}$ are incoming and outgoing lepton momenta; q is the photon momentum.

Feynman amplitudes of different types (a type is the set of the external line types); the linear operators under the same symbol U_j for different types can be chosen independently. Of course, U_j can be chosen independently for different j. U_1 and U_3 are defined only for the Feynman amplitudes with the external leptons coinciding with those whose AMM is calculated; U_2 are defined for all types of external leptons (for example, it can be chosen independently for the

Feynman amplitudes with external electrons, muons, and tau-leptons).

The expression for the subtraction and extraction of the AMM corresponding to a Feynman graph G is

$$\sum_{\substack{F=\{G_1,\ldots,G_n\}\in \mathfrak{F}[G]\\ G'\in \mathcal{I}[G]\cap F}} (-1)^{n-1} S_{G_1}^{G'}\ldots S_{G_n}^{G'},$$

where

$$S_{G''}^{G'} = \begin{cases} A_{G''}, & \text{if } G'' = G', \\ L_{G''} - (U_1)_{G''}, & \text{if } G'' = G \neq G', \\ L_{G''}, & \text{if } G' \subset G'' \subset G, \\ (U_\xi)_{G''}, & \text{if } G'' \in \mathcal{I}[G] \text{ and } G'' \subset G', \\ (U_1)_{G''}, & \text{if } G'' \notin \mathcal{I}[G] \text{ and } G'' \text{ has its external leptons on the main path of } G, \\ (U_2)_{G''}, & \text{if } G'' \text{ has its external leptons on a lepton loop of } G, \\ (U_0)_{G''}, & \text{if } G'' \text{ is a photon self-energy or photon-photon scattering subgraph}; \end{cases}$$

here,

$$\xi = \begin{cases} 3, & \text{if the vertex incident to the external photon of the whole graph } G \text{ lies on a lepton loop of } G, \\ 1 & \text{otherwise}; \end{cases} \quad (15)$$

the index of an operator denotes the subgraph to whose Feynman amplitude it is applied; $G_1 \subset G_2$ or $G_1 \subseteq G_2$ means $V(G_1) \subset V(G_2)$ or $V(G_1) \subseteq V(G_2)$, where $V(G)$ denotes the set of vertices of G. We emphasize that the whole graph G is used in the definition of ξ; thus, ξ does not depend on G' and G''. At the level of Feynman amplitudes, each term of the expression sequentially transforms the Feynman amplitudes of subgraphs using corresponding linear operators (the subgraphs should be ordered by inclusion in this sequence, from smaller to larger). Finally, the coefficient before γ_μ should be taken.

For example, for the graph G from Fig. 1 the expression is

$$[A_G(1 - (U_3)_{G_e}) - (L_G - (U_1)_G)A_{G_e}] \times (1 - (U_2)_{G_c})$$
$$\times (1 - (U_1)_{e_2e_4e_5})(1 - (U_0)_{G_d}) \times (1 - (U_0)_{c_1c_2c_3c_4})$$
$$\times (1 - (U_2)_{c_1c_2c_3} - (U_2)_{c_1c_3c_4}) \times (1 - (U_2)_{a_1a_2}),$$

where $G_e = aa_1a_2b_1b_2c_1c_2c_3c_4d_1d_2d_3e_1e_2e_3e_4e_5$, $G_d = \{aa_1a_2b_1b_2c_1c_2c_3c_4d_1d_2d_3\}$, $G_c = aa_1a_2b_1b_2c_1c_2c_3c_4$, $\mathcal{I}[G] = \{G_e, G\}$, subdiagrams are denoted by enumeration of their internal vertices; we should expand the parentheses to obtain the forest formula. The expression for this example does not depend on the type of leptons on the lepton loops (U_2 may be defined differently for different types of leptons, however).
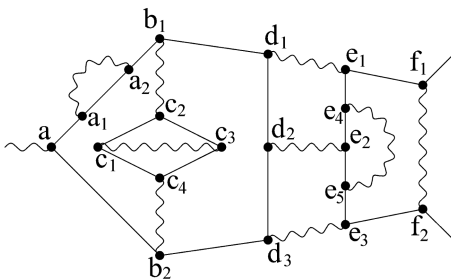

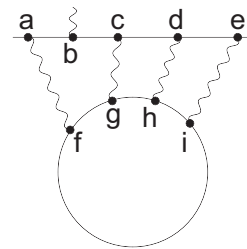FIG. 1. An example of a Feynman diagram contributing to AMM.

FIG. 2. Another example of a Feynman diagram contributing to AMM.

Another example is the graph G from Fig. 2. In this case, $\mathcal{I}[G] = \{G\}$, the expression is

$$A_G(1 - (U_1)_{cdefghi})(1 - (U_0)_{fghi}).$$

The operator U_1 is applied to the subgraph $cdefghi$, because its external leptons are on the main path of G.

To obtain finite Feynman parametric integrals, all terms should be placed in the same Feynman parametric space. The algorithm for obtaining integrals from expressions is briefly explained in [71] and in detail in [69]. The needed value of $A_l^{(2n)}$ is simply the sum of the integrals corresponding to the Feynman graphs involved.

III. DIVERGENCE ELIMINATION

The principle of divergence elimination in the method is similar to that explained in [69] for the old method. Here, we describe schematically how this choice of linear operators allows us to separate divergences and how it leads to divergence cancellation.

Let us consider the 1-loop unrenormalized vertexlike Feynman amplitude,[13]

$$\Gamma_{1,\mu}(p,q) = \int \gamma^\nu \frac{\not{p} + \frac{\not{q}}{2} + \not{k} + m}{(p + \frac{q}{2} + k)^2 - m^2 + i0}$$

$$\times \gamma_\mu \frac{\not{p} - \frac{\not{q}}{2} + \not{k} + m}{(p - \frac{q}{2} + k)^2 - m^2 + i0} \gamma_\nu \frac{1}{k^2 + i0} d^4k.$$

Its IR-divergent part at $p^2 = m^2$ is equal to

$$\Gamma_{1,\mu}(p,0)_{\text{IR}} = \left[\int \gamma^\nu \frac{\not{p} + m}{(p + k)^2 - m^2 + i0} \right.$$

$$\left. \times \gamma_\mu \frac{\not{p} + m}{(p + k)^2 - m^2 + i0} \gamma_\nu \frac{1}{k^2 + i0} d^4k \right]_{\text{IR}}.$$

With

$$(\not{p} + m)\gamma_\mu(\not{p} + m) = 2mp_\mu + 2p_\mu\not{p}$$

and the fact that p_μ commutes with all other multipliers that may appear in the expression, we obtain

$$\Gamma_{1,\mu}(p,0)_{\text{IR}} = Ap_\mu + Bp_\mu\not{p},$$

where A and B some IR-divergent values.[14] Thus, $U_1\Gamma_1$ and $U_2\Gamma_1$ are IR-finite. On the other hand, the UV-divergent part of $\Gamma_{1,\mu}(p,q)$ does not depend on p, q
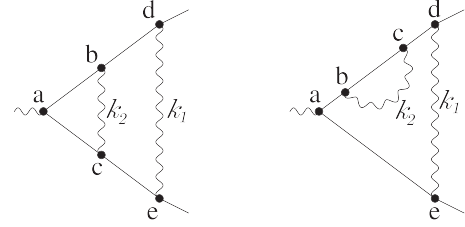

FIG. 3. 2-loop examples.

and is therefore proportional to γ_μ. Thus, $(L - U_j)\Gamma_1$, $j = 1, 2$ are UV-finite.

There is a general observation:
(i) $(L - U_j)\Gamma$, $j = 1, 2, 3$ has no *overall* UV divergence for any vertexlike Feynman amplitude Γ (of any order);
(ii) $U_j\Gamma$, $j = 1, 2$ does not have IR divergences at all, provided that the mass renormalization has been done properly (see below);
(iii) this is also true for $U_j\Sigma$, $j = 1, 2$, where Σ is a lepton self-energy Feynman amplitude.

In particular, this means that U_1, U_2 can be used to subtract UV divergences without generating additional IR divergences (unlike L).

Consider the 2-loop ladder graph G in Fig. 3, left.[15] The corresponding expression is

$$A_G - A_G(U_1)_{abc} - (L - U_1)_G A_{abc}.$$

In this case, we have only logarithmic divergences. The overall UV divergence corresponds to $k_1, k_2 \to \infty$; it is proportional to γ_μ and is cancelled in each term by A or $L - U_1$. The overall IR divergence corresponds to $k_1, k_2 \to 0$. In all terms, it is canceled by A since it is proportional to the Born amplitude $(A\gamma)_\mu = 0$, where by γ we denote the 4-vector of Dirac gamma matrices; this can be shown using standard methods for studying IR divergences in QED. There is also a mixed UV-IR divergence in this graph: $k_1 \to 0, k_2 \to \infty$; in this case, the UV divergence corresponding to abc is IR-infinitely enhanced by the remaining propagators. In the first two terms, it is canceled by A, because the UV-divergent part of abc is proportional to γ_μ, so the "enhanced" value is proportional to $(A\gamma)_\mu = 0$. In the remaining term, it is canceled in A_{abc} for the same reason. The remaining divergences[16] are the UV divergence $k_2 \to \infty$ and the IR divergence $k_1 \to 0$. The first is canceled in the sum of two terms by

---

[13]We ignore coefficients in this consideration.
[14]We mean that a regularization is introduced, but we omit it for simplicity.

[15]Since changing the lepton line directions on a path or loop does not change the contribution, we will sometimes work with undirected Feynman graphs.
[16]This investigation is intended to demonstrate ideas only; a rigorous proof is not the goal in this case.

$1 - U_1$ applied to the amplitude of abc and in the last term by A_{abc}. The second does not exist in $A_G(U_1)_{abc}$, in A_G, it enhances the amplitude generated by A_{abc} by an IR-infinite multiplier, and it is canceled by $(L - U_1)_G A_{abc}$, because $L - U_1$ completely extracts the IR-divergent part of the enhancing multiplier.

Let us examine the graph G on Fig. 3, right. The expression is

$$A_G - A_G(U_1)_{bc}.$$

The difficulty in this case is the power-type IR-divergence corresponding to $k_1 \to 0$ and a fixed $k_2 \neq 0$. However, it is eliminated by the mass subtraction part in U_1. To make this possible, we give no freedom to the definition (14) of M' in (12). After the mass subtraction, the IR divergence becomes logarithmic and is removed by A, as is the overall UV divergence. The UV subdivergence of bc is removed by $1 - U_1$, and no additional IR divergence is generated.

Let us consider the graph G on Fig. 4. The expression is

$$[A_G - A_G(U_3)_{bcdfghi} - (L - U_1)_G A_{bcdfghi}](1 - (U_0)_{fghi}).$$

The last multiplier eliminates the UV divergence corresponding to $fghi$; in this case, there are no problems with IR divergences. The last term of the first multiplier removes the IR divergence corresponding to $k_{ae} \to 0$ (the subscript denotes the graph line by its ends). The term $A_G(U_3)_{bcdfghi}$ removes the UV divergence corresponding to $bcdfghi$. It is important to note that it does not create any additional IR divergence, although U_3 has more freedom in definition than U_1 and U_2 (we can take $U_3 = L$, for example). The reason is that the on shell Feynman amplitude of $bcdfghi$ has no IR divergence, because its external photon is on a lepton loop.

The cancellation of divergences in Feynman parametric space for an arbitrary graph G can be shown in a similar way as in [69], but U should be replaced everywhere by the corresponding U_j. Let us note one more small change.
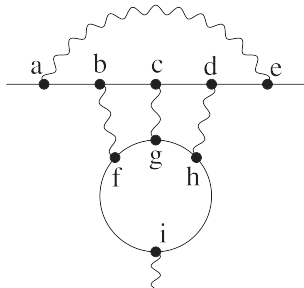

FIG. 4.   An example with U_3 in the expression.

Following [69], Appendix C, we assume that $G_1 \subset \ldots \subset G_n \subset G_{n+1} = G$ are all elements of $\mathcal{I}[G]$. If $\xi = 1$, where (15) is implied, we also assume that G_0 is the graph consisting of only one vertex of G joining the external photon (if $\xi = 3$, we use G_0 as the empty graph). By z_l we denote the Feynman parameter corresponding to the internal line l. With the help of power counting, we investigate the case,

$$z_l \asymp \delta^{\beta_l}, \delta \to 0,$$

where $\beta_l \geq 0$ are some numbers corresponding to the internal lines. By P_j, we denote[17] the set of all lines l on the main path of G such that $l \in G_{j+1}$ and $l \notin G_j$. The cancellation of UV divergences and UV parts of mixed divergences is demonstrated in the same way[18] as in [69]. If all divergences not belonging to $\mathcal{I}[G]$ are properly subtracted, a potentially IR divergent case corresponds to a *vector of divergences* $[v_0, \ldots, v_n; w_0, \ldots, w_n]$, where $v_j \geq w_j \geq 0$, $2v_0 - w_0 = 2v_1 - w_1 = \ldots = 2v_n - w_n > 0$, there exists j such that $w_j = 0$. This vector gives the values,

$$\beta_l = \begin{cases} v_j, & \text{if } l \in P_j, \\ w_j, & \text{if } l \in G_{j+1}, j \notin G_j, j \notin P_j. \end{cases}$$

We will refer to the index j, $1 \leq j \leq n$ as a *transition index* for the divergence vector $[v, w]$ if $v_j > v_{j-1}$. Correspondingly, the index j is called an *inverse transition index* if $v_j < v_{j-1}$. The difference with the investigation in [69] is the following:

(1) An index j is called *separating* in a term of the expression if there is an operator A_{G_j}, L_{G_j} or $(U_3)_{G_j}$ $(U_3 = L)$ in this term. The difference with [69] is the possibility to take U_3 (if it is equal to L).

(2) If $\xi = 3$, then no consideration of the case $v_0 > w_0$ is necessary; this case cannot produce divergence in a term, because G_1 has its external photon on a lepton loop.

(3) If $\xi = 3$ and $U_3 = L$, we rewrite the expression differently for a given index H of the inverse transition in $[v, w]$,

---

[17]In [69], it is denoted by $P'_j \cup P''_j$.

[18]The expression is organized in a very similar way to Zimmermann's forest formula; this makes it possible to handle UV divergences.

$$- \sum_{1 \le l < H} (L_G - (U_1)_G)(1 - L_{G_n})...(1 - L_{G_{l+1}})A_{G_l}(1 - L_{G_{l-1}})...(1 - L_{G_1}))$$

$$+ \sum_{H < l \le n} ((L_G - (U_1)_G)(1 - L_{G_n})...(1 - L_{G_{l+1}})[L_{G_l}A_{G_H} - A_{G_l}](1 - L_{G_{H-1}})...(1 - L_{G_1}))$$

$$+ [A_G - (L_G - (U_1)_G)A_{G_H}](1 - L_{G_{H-1}})...(1 - L_{G_1})$$

$$+ \sum_{H < l \le n} \left[\left(A_G(1 - L_{G_n})...(1 - L_{G_{l+1}}) - (L_G - (U_1)_G) \sum_{l < k \le n} \left(A_{G_k} \prod_{\substack{l < r \le n \\ r \ne k}} (1 - L_{G_r}) \right) \right) \right.$$

$$\left. \times [L_{G_l}L_{G_H} - L_{G_l}](1 - L_{G_{H-1}})...(1 - L_{G_1}) \right].$$

The last term was added to (C.7) in [69], inappropriate $(1 - U)$ multipliers were removed. The factor $L_{G_l}L_{G_H} - L_{G_l}$ cancels the divergence in this term, analogous to the other terms.

This argument shows how it works, but a full rigorous examination seems difficult and cumbersome; we rely on a numerical check (see Sec. V).

IV. EQUIVALENCE TO ON-SHELL RENORMALIZATION

A. Definition

The definition of on shell renormalization is well known for the coefficients of the expansion in α, but it requires a definition for subsets of Feynman graphs. We define it as the sum of the individual graph contributions obtained by the in-place on shell renormalization. It can be written in terms of expressions such as those used above. The expression for a graph G is

$$\sum_{F = \{G, G_1, ..., G_n\} \in \mathfrak{F}[G]} (-1)^n A_G S_{G_1}...S_{G_n},$$

where

$$S_{G'} = \begin{cases} L_{G'}, & \text{if } G' \text{ is a vertexlike graph,} \\ B_{G'}, & \text{if } G' \text{ is a lepton self-energy graph,} \\ (U_0)_{G'}, & \text{if } G' \text{ is a photon self-energy or photon-photon scattering graph;} \end{cases}$$

here,

$$(B\Sigma)(p) = [B'\Sigma] \times (\not{p} - m) + M'\Sigma,$$

$$B'\Sigma = s(m^2) + 2m \frac{\partial r(x)}{\partial x}\bigg|_{x=m^2} + 2m^2 \frac{\partial s(x)}{\partial x}\bigg|_{x=m^2},$$

where (13) and (14) are satisfied.

The multipliers $S_{G'}$ for photon-photon scattering graphs G' can be omitted in gauge-invariant classes as well as transformations like described in [72] can be applied for photon self-energy graphs.

B. Examples

Two-loop examples are given in [69] for the old version of the method. In the new version, each operator U should be replaced by U_1 or U_0.

The Ward identities for individual Feynman graphs play an important role in proving the equivalence. We will illustrate this by the gauge-invariant class shown in Fig. 5. The investigation applies to both the new and old methods (the difference is only in the name of the U-operator).

Table I provides the parts of the contributions, obtained with our method, that contain U-operators. The lower-order Feynman amplitudes used in these expressions are shown in Fig. 6. The boxed dots represent the mass vertices (the vertices that give 1 in the Feynman rules). By Γ_1 and Σ_1, we also denote the 1-loop vertexlike and lepton self-energy amplitudes (without special vertices), respectively. In this
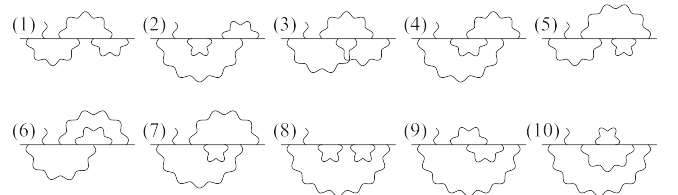

FIG. 5. An example of a 3-loop gauge-invariant class.

TABLE I. Contributions with U-operators of the graphs from Fig. 5 obtained with our method.

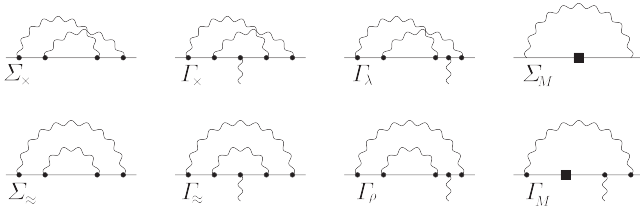| Set number	Contribution
1	$-(A'\Gamma_1)(U'_1\Gamma_\lambda) - (A'\Gamma_\lambda)(U'_1\Gamma_1) + (A'\Gamma_1)(U'_1\Gamma_1)^2$
2	$-(A'\Gamma_\rho)(U'_1\Gamma_1) - (A'\Gamma_\lambda)(U'_1\Sigma_1) + (A'\Gamma_1)(U'_1\Gamma_1)(U'_1\Sigma_1) + (A'\Gamma_M)(U'_1\Gamma_1)(M'\Sigma_1)$
3	$-(A'\Gamma_1)(U'_1\Gamma_\times)$
4	$-(A'\Gamma_1)(U'_1\Gamma_\lambda) - (A'\Gamma_\lambda)(U'_1\Gamma_1) + (A'\Gamma_1)(U'_1\Gamma_1)^2$
5	$-(A'\Gamma_1)(U'_1\Gamma_\rho) - (A'\Gamma_\lambda)(U'_1\Sigma_1) + (A'\Gamma_1)(U'_1\Gamma_1)(U'_1\Sigma_1) + (A'\Gamma_1)(U'_1\Gamma_M)(M'\Sigma_1)$
6	$-(A'\Gamma_1)(U'_1\Gamma_\approx) - (A'\Gamma_\lambda)(U'_1\Gamma_1) + (A'\Gamma_1)(U'_1\Gamma_1)^2$
7	$-(A'\Gamma_1)(U'_1\Gamma_\rho) - (A'\Gamma_\lambda)(U'_1\Sigma_1) + (A'\Gamma_1)(U'_1\Gamma_1)(U'_1\Sigma_1) + (A'\Gamma_1)(U'_1\Gamma_M)(M'\Sigma_1)$
8	$-2(A'\Gamma_\rho)(U'_1\Sigma_1) + (A'\Gamma_1)(U'_1\Sigma_1)^2 + 2(A'\Gamma_M)(U'_1\Sigma_1)(M'\Sigma_1)$
9	$-(A'\Gamma_1)(U'_1\Sigma_\times) - 2(A'\Gamma_\rho)(U'_1\Gamma_1) + 2(A'\Gamma_1)(U'_1\Sigma_1)(U'_1\Gamma_1) + 2(A'\Gamma_M)(M'\Sigma_1)(U'_1\Gamma_1)$
10	$-(A'\Gamma_1)(U'_1\Sigma_\approx) - (A'\Gamma_\rho)(U'_1\Sigma_1) + (A'\Gamma_1)(U'_1\Sigma_1)^2 + (A'\Gamma_M)(M'\Sigma_1)(U'_1\Sigma_1) + (A'\Gamma_1)(U'_1\Sigma_M)(M'\Sigma_1)$

FIG. 6. Feynman amplitudes participating in the expressions for the set in Fig. 5 and the corresponding Feynman graphs.

case, $\mathcal{I}[G] = \varnothing$, and we have no IR subtractions; therefore, the remaining contributions are the same as those obtained by the in-place on-shell renormalization.

After summation, we obtain

$$(A'\Gamma_1)(-[2U'_1\Gamma_\lambda + U'_1\Gamma_\times + U'_1\Sigma_\times]$$
$$- [2U'_1\Gamma_\rho + U'_1\Gamma_\approx + U'_1\Sigma_\approx])$$
$$+ [U'_1\Gamma_1 + U'_1\Sigma_1](-3A'\Gamma_\lambda - 3A'\Gamma_\rho$$
$$+ (A'\Gamma_1)(3U'_1\Gamma_1 + 2U'_1\Sigma_1))$$
$$+ (A'\Gamma_1)(M'\Sigma_1)[2U'_1\Gamma_M + U'_1\Sigma_M].$$

We use the following Ward identities for individual graphs:

$$(\Gamma_1)_\mu(p,0) + \frac{\partial\Sigma_1(p)}{\partial p^\mu} = 0, \qquad 2(\Gamma_M)_\mu(p,0) + \frac{\partial\Sigma_M(p)}{\partial p^\mu} = 0,$$

$$2(\Gamma_\lambda)_\mu(p,0) + (\Gamma_\times)_\mu(p,0) + \frac{\partial\Sigma_\times(p)}{\partial p^\mu} = 0,$$

$$2(\Gamma_\rho)_\mu(p,0) + (\Gamma_\approx)_\mu(p,0) + \frac{\partial\Sigma_\approx(p)}{\partial p^\mu} = 0.$$

Each identity contains one lepton self-energy graph and all vertexlike graphs obtained by inserting an external photon into a line on the main path. Each coefficient equals 1, but
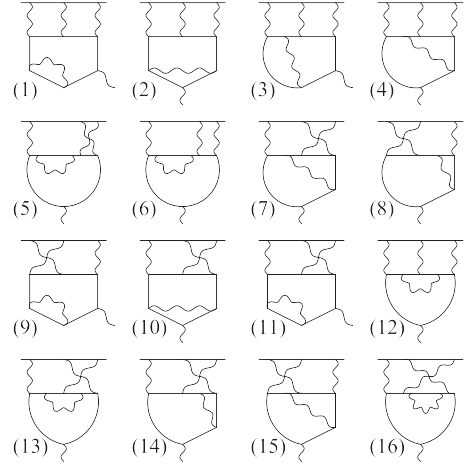
FIG. 7. 4-loop gauge-invariant class IV(b) from [52].

some of our coefficients equal 2, because we are working with undirected Feynman graphs. The identities can be proved by standard methods used in QED.[19] The corollary is

$$U'_1\Gamma_1 + U'_1\Sigma_1 = 0, \qquad 2U'_1\Gamma_M + U'_1\Sigma_M = 0,$$
$$2U'_1\Gamma_\lambda + U'_1\Gamma_\times + U'_1\Sigma_\times = 0,$$
$$2U'_1\Gamma_\rho + U'_1\Gamma_\approx + U'_1\Sigma_\approx = 0.$$

From this, it follows that all terms with U'_1 are canceled. Similarly, we can prove that all terms with L' and B' are lifted in the on shell expression, which implies the equivalence.[20]

Let us examine examples where the new and old methods work differently. We start with the 4-loop class IV(b) from Fig. 7. We suppose that the graphs contribute to the muon $g - 2$ and contain an electron loop.

---

[19]See [73].
[20]provided that all regularization issues are resolved; dimensional regularization can be used in most cases.
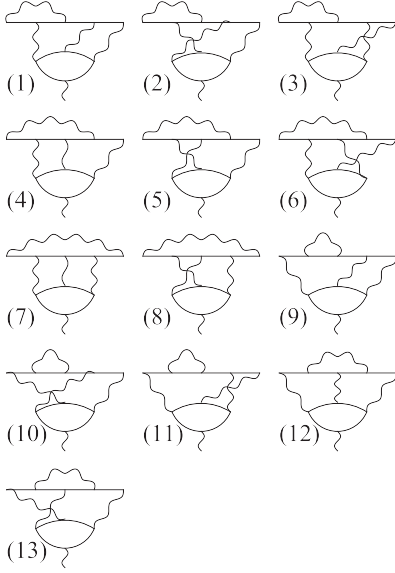
FIG. 8. 4-loop gauge-invariant class IV(c) from [52].

The difference is that the old method yields additional subtractions in graphs 2,10 because each of them has a vertexlike subgraph joining the external photon and not lying on the main path.[21] Also, the operators U_2 are used everywhere instead of U. The contribution of IV(b) is equal to

$$(-8A'[\text{⊟}_e] - 16A'[\text{⊟}_e]) \ (U_2'[\text{△}_e] + U_2'[\text{◠}_e])$$
$$\begin{aligned}&+(\text{terms with A only})\\&+(\text{terms with light--by--light operators})\\&+(\text{remaining terms with mass parts})\end{aligned}$$

The first term is canceled because its second multiplier equals 0 due to the Ward identity; the light-by-light term is similar and is canceled for the same reason. The expression for the on shell renormalization has the same form, but the occurrences of U_2' are replaced with L', B'; its terms already considered are canceled due to the same reason. The remaining terms are identical.

Consider the class IV(c) from Fig. 8. In this case, we also assume that the graphs contribute to the muon $g-2$ and have an electron loop. Graphs 7 and 8 give terms with U_3. The total contribution of these graphs is

$$-A'[\text{△}](2U_3'[\text{⊟}_e] + 4U_3'[\text{⊟}_e])$$
$$-(L'-U_1')[\text{△}](2A'[\text{⊟}_e] + 4A'[\text{⊟}_e])$$

---

[21]These subgraphs correspond to fictitious IR divergences, but the subtraction was necessary in [69] to make the procedure equivalent to on shell renormalization.

We ignore the terms with U_0' and M' in this investigation, because they do not cause any problems. To show that the first term equals 0, we need the Ward identities of the form $\Gamma_\mu(p,0) = 0$ for single graphs. It holds for sets of vertex-like graphs that have the external photon on a *lepton loop* that are closed under the movement of it along the loop. The validity can be proved in the usual way. Since U_3 preserves this kind of Ward identities, its contributions are cancelled. The remaining graphs yield

$$-A'[\text{⊟}_e](6U_1'[\text{△}] + 4U_1'[\text{◠}])$$
$$-A'[\text{⊟}_e](12U_1'[\text{△}] + 8U_1'[\text{◠}])$$

With $U_1'\Gamma_1 = -U_1'\Sigma_1$, we get that all terms containing U_1' are canceled after summation. The total contribution obtained by the in-place on shell renormalization is

$$-A'[\text{△}](2L'[\text{⊟}_e] + 4L'[\text{⊟}_e])$$
$$-(A'[\text{⊟}_e] + 2A'[\text{⊟}_e])(6L'[\text{△}] + 4B'[\text{◠}])$$

The difference between our and on shell contributions equals

$$(4A'[\text{⊟}_e] + 8A'[\text{⊟}_e])(L'[\text{△}] + B'[\text{◠}]).$$

It equals 0, because $L'\Gamma_1 = -B'\Sigma_1$.

Let us summarize. To prove the equivalence, we need two kinds of the "Ward identities" for single graphs:

(i) $\Gamma_\mu(p,0) = -\partial\Sigma(p)/\partial p^\mu$; the set includes one lepton self-energy graph and all vertexlike graphs obtained from it by inserting an external photon into a line on the main path.

(ii) $\Gamma_\mu(p,0) = 0$; the set consists of vertexlike graphs having the external photon on a lepton loop; it is closed under the movement of the external photon along the loop.

Graphs in the sets may contain special vertices. See also examples of the use of the Ward identities for individual graphs in Sec. IV.H of [32].

C. Complete proof

Suppose we have a class $\mathcal{K}$ of *1-particle irreducible* vertexlike Feynman graphs that is closed under the movement of internal photons along lepton loops and paths, but without jumping over the external photon. We prove that its contribution obtained with our method is equal to the contribution obtained with the in-place on shell renormalization. Since the ideas used here are similar to those widely used in QED, the explanation is just a framework.

Let us give some definitions.

Suppose we have one term X of the expression with linear operators constructed for some graph G of this class. The subgraphs to which the operators in X are applied form a rooted tree; in this tree, G is a root, and G' is a descendant of G'' if $G' \subset G''$. The contribution of X can be expressed with A', U'_j, L', $L' - U'_j$, M', B' applied to some graphs with special vertices. This expression can have several terms $Y_1, ..., Y_n$, because $U_j\Sigma$ is split into U'_j-part and M'-part. Each term Y_j can be represented as a *layer tree*. A *layer* is a Feynman graph obtained from one graph to which an operator in X is applied by shrinking all its childs to special vertices (corresponding to operators in Y). A layer tree is a rooted tree, each node of it is (l, O, r), where l is a layer; O is one of the operators A', U'_j, L', $L' - U'_j$, M', B'; r is the reference to the corresponding vertex of the parent (it does not exist for the root). The root of the layer tree corresponds to G in X. Vertices and inputs of one vertex that have the same type are enumerated.[22] The contribution of the layer tree (without coefficient) is the product of the node values,[23] where the value of the node (l, O, r) is $O\Gamma_l$, where Γ_l is the Feynman amplitude corresponding to the layer l. For simplicity, we will sometimes interchange the layer tree nodes with the layers.

For example, the term $A_G(U_0)_{defghi}(U_2)_{gh}$ for the graph G from Fig. 9, left gives the layer tree depicted in Fig. 9, right.

The following markers are used for vertices on images:
(1) a round dot is an ordinary γ_ν vertex;
(2) a boxed dot is a mass vertex (which gives 1);
(3) a cross-dot is a $(\not{p} - m)$-vertex;
(4) a cross in a circle is a vertex coming from photon self energy subgraphs;
(5) a diamond dot is a vertex originating from photon-photon scattering subgraphs.

Another example is the term,

$$A_G B_{bcdefghi} L_{cdefg} B_{de} B_{klno}(U_0)_{no}$$

for G from Fig. 10, left, where M' parts are taken for each B (the term is part of the direct on shell renormalization expression). Its layer tree is depicted in Fig. 10, right. The root is layer 1.

---

[22]The enumeration is needed to avoid symmetry problems with 4-photon vertices. If we have an enumeration, the coefficients should be properly accounted for; this can be done with a standard technique; we do not do this in our consideration. An examination of the coefficients is only necessary for symmetry issues; no reduction of similar terms takes place in our consideration.

[23]Strictly speaking, tensor contractions are needed when we have U'_0 layers, because for simplicity, we decided to use one label for all kinds of special vertices that can be generated. For example, in the definition (9), (10) for photon self-energy graphs, U'_0 is a vector.
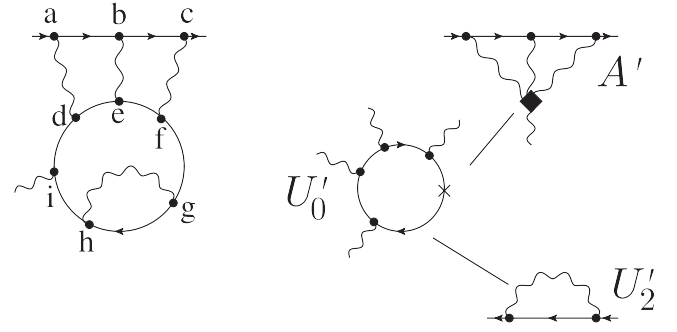

FIG. 9. An example of a Feynman graph (left) and a layer tree (right) that is possible for it (with U'_0 and U'_2 for lepton self-energy graphs).

The sequence of layer tree nodes $Y_1, ..., Y_n$ of vertexlike type is called the *main branch* if the following conditions are satisfied:
(i) Y_1 is the root of the layer tree;
(ii) Y_{j+1} is the child of Y_j corresponding to the vertex of Y_j joining its external photon;
(iii) Y_n has no vertexlike children corresponding to its vertex joining its external photon;
the *type* of a layer is its multiset of the external line types.

We say that the node X of a layer tree is *locally on a path*, if the corresponding to X parent's vertex lies on parent's main path; we also assume that the root of the layer tree is locally on a path. If the node is not locally on a path, it may be on a loop or on a special 2-photon or 4-photon vertex of the parent.

The maximal initial segment $Y_1, Y_2, ..., Y_k$ of the main branch $Y_1, Y_2, ..., Y_n$, all elements of that are locally on a path, is called the $\mathcal{I}$-*branch*.

Let us proceed with the proof. We represent the contribution of $\mathcal{K}$ obtained by our method as the sum of the layer tree contributions (with coefficients). Each layer tree has one node X on the $\mathcal{I}$-branch that has the operator A'. We call it the *A-node*. The operators corresponding to vertexlike or lepton self-energy nodes X satisfy the following rules:
(i) if X is the A-node, then the corresponding operator is A';
(ii) if X is the root but not A-node, then the operator is $L' - U'_1$;
(iii) if X is an ascendant of the A-node but not the root, then the operator is L;
(iv) if X is a descendant of the A-node and belongs to the $\mathcal{I}$-branch, then the operator is U_ξ, where (15) is satisfied for graphs G in $\mathcal{K}$;
(v) if X is not on the $\mathcal{I}$-branch and all ascendants of X and X itself are locally on a path, then the operator is U'_1 or M';
(vi) if X is not on the $\mathcal{I}$-branch and at least one ascendant of X or X itself is not locally on a path, then the operator is U'_2 or M'.
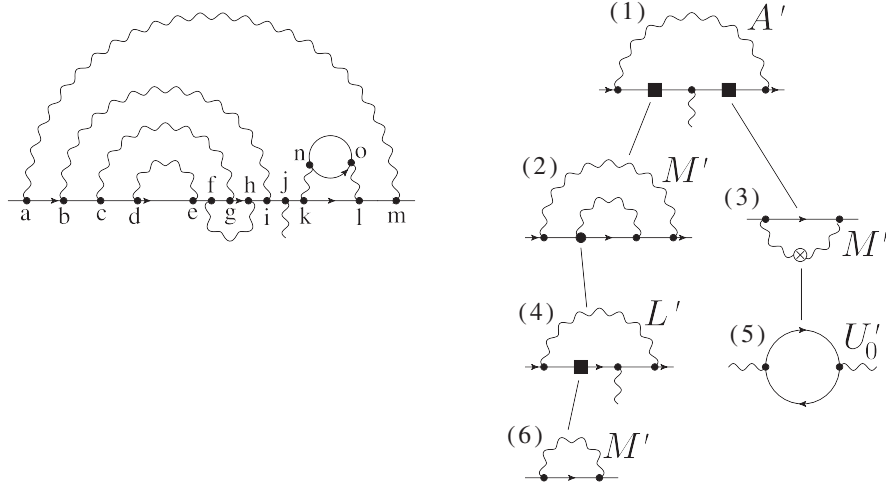
FIG. 10. An example of a Feynman graph (left) and a possible layer tree for it (right) with M'-operators.

Let us perform the following operations with this layer tree sum:

(1) *Remove all terms containing layers of photon-photon scattering type*. In fact, they are canceled by the identities for individual photon-photon scattering graphs of the form,

$$\Gamma_{\mu_1\mu_2\mu_3\mu_4}(0,0,0,0) = 0,$$

where Γ is the corresponding Feynman amplitude, and the external momenta are in the parentheses. The identity is satisfied for a given set of graphs, if the set is closed under the movement of external photons along lepton loops, and *every graph in this set contains at least one external photon line joining a lepton loop* (we consider graphs with special vertices; thus, an external photon can fall into a 4-photon vertex). The identities can be proved with a standard technique that is used in QED.[24] Let us consider the elimination in detail. We say that the layer trees T_1 and T_2 are equivalent if one is obtained from the other by the movement of external photons along lepton loops in some layers of photon-photon scattering types, *which have no descendants of photon-photon scattering type* (the absence of the descendants guarantees that all moved photons are on lepton loops[25]); we suppose that the structure of the descendants is preserved when a photon is shifted; the children referring to the vertex joining the moved photon change their reference to the new photon location on a lepton loop. It is easy to see that if T_1 is obtained from a Feynman graph of $\mathcal{K}$, this is also true for T_2. Therefore, all terms are split into equivalence classes. In the contribution of each of these classes, the identities mentioned above are factorized. This leaves only the classes that have no photon-photon scattering layers at all. Note that the movement of photons (both external and internal) along lepton loops does not change the 1-particle irreducibility.

(2) *Remove all terms containing vertexlike layers with a non-A' operator and the external photon on a loop.*[26] The operator is L', U'_1, U'_2, U'_3. All these operators yield 0 for the Feynman amplitudes $\Gamma_\mu(p,q)$ satisfying $\Gamma_\mu(p,0) = 0$. Thus all these terms are cancelled by the identities of this form mentioned in Sec. IV B. This can be proved in a similar way as for the case with photon-photon scattering layers. After this step, all occurrences of U'_3 are removed, since at least the U'_3 corresponding to the end of the $\mathcal{I}$-branch is applied to a layer with the external photon on a lepton loop.

(3) *Represent the layer trees as trees of M-blocks*. An *M-block* includes a node (vertexlike or lepton self-energy-like) with an operator A', L', U'_j ($j = 1, 2$) of the layer tree, all its children with operators M', U'_0, their children with these operators and so on.[27] For example, there are two M-blocks in 10, right: $\{1, 2, 3, 5\}$ and $\{4, 6\}$; the latter is a child of the former and refers to the vertex of layer 2 to which layer 4 refers. M-blocks can also be represented as layers. The layer is obtained from the corresponding subgraph by shrinking the subgraphs corresponding to its children (in the tree of M-blocks) to special vertices (in a sense, it is obtained by gluing the layer

---

[24]See [73].

[25]They cannot fall to 2-photon vertices due to 1-particle irreducibility.

[26]We consider here only the internal structure of the layer, not its reference to its parent.

[27]We do not use here that M' properly extracts the mass part, but it is used for the proof of gauge invariance [8].

tree layers belonging to the M-block). An M-block can also be viewed as a tree of nodes. Let us define the *main vertex* of the M-block; if the layer has its external photon on its main path, the main vertex is layer's vertex joining its external photon; otherwise, it is the *last vertex of the main path* of the layer.

(4) *Single out the $\mathcal{S}$-branch of M-blocks in each layer tree*. We define the $\mathcal{S}$-branch of M-blocks $Y'_1, \ldots, Y'_n$ in a tree of M-blocks by the following conditions:
 (i) Y'_1 is the root of the M-block tree;
 (ii) Y'_j, $j \geq 2$, is a child of Y'_{j-1} and refers to the main vertex of Y'_{j-1};
 (iii) there are no children of Y'_n that refer to the main vertex of Y'_n.
 An initial segment $Y'_1, \ldots, Y'_k$ of the $\mathcal{S}$-branch corresponds to the $\mathcal{I}$-branch $Y_1, \ldots, Y_k$. Due to the 1-particle irreducibility of each subgraph to which an operator is applied, all elements of the $\mathcal{S}$-branch are of vertexlike type.

(5) *For each M-block take a one-to-one correspondence between the layer vertices (except the main vertex) and its Σ-chains lying on the same lepton path part or loop*. A Σ-*chain* is a peace of a lepton path or loop, which ends are ordinary γ_μ vertices, but all intermediate vertices are of $(\not{p} - m)$ type (the situation when there are no intermediate vertices is also possible). We require that the Σ-chain lies on the same side of the M-block external photon as the corresponding vertex (if it is applicable). We should take this correspondence *deterministically* (it should depend only on the topology of the Σ-chains and external lines). For example, for each v on a lepton loop, we can take the outgoing from v chain; for v on the main path, we can take the Σ-chain joining v and having another end closer to the main vertex of the M-block.

(6) *Remove all terms containing M-blocks outside the $\mathcal{S}$-branch*. Let us explain how they are canceled. An M-block is called *factorizable* if it has at least one child that does not refer to its main vertex. We say that the M-block trees $\mathcal{T}_1$ and $\mathcal{T}_2$ are equivalent if one is obtained from the other by a sequence of the following transformations:
 (i) suppose Y' is a factorizable M-block that *has no factorizable children*, v is an ordinary γ_μ-vertex in Y', the main vertex of Y' is not equal v, the Σ-chain σ corresponds to v, the child M-block referring to v exists and is denoted by Y''; the transformation is: remove the external photon in the *root layer* of Y'', move the reference of Y'' to the new $(\not{p} - m)$ vertex inserted at the beginning of σ; the operator applied is U'_j, $j = 1, 2$ and remains the same after the transformation; the structure of the descendants and their references are preserved, *the reference to the main*
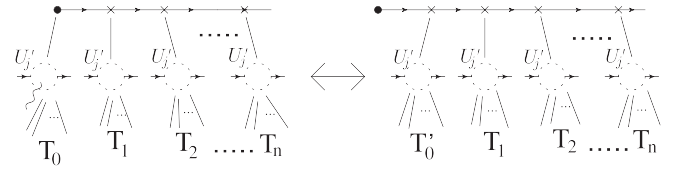

FIG. 11. Transformations leading to the cancellation of all terms with M-blocks outside the $\mathcal{S}$-branch.

vertex of Y'' is moved to the main vertex of the transformed M-block (there are no references to nonmain vertices, since Y' has no factorizable children).
 (ii) if under the same conditions there are no children referring to v, and the intermediate vertexes of σ are $w_1, \ldots, w_r$, $r \geq 1$ (ordered along the line direction), Y'' is the child M-block referring to w_1, then insert an external photon into an arbitrary line on the main path of the *root layer* of Y'', remove w_1 and move the reference of Y'' to v. The applied operator is U'_j, $j = 1, 2$ and remains the same after the transformation; the structure of the descendants and their references are preserved (as in the previous case).

These transformations are inverse to each other. They are illustrated in Fig. 11; here, v is the round dot, σ starts from v, T_0 is a subtree referring to v in the layer tree, the subtrees $T_1, \ldots, T_n$ refer to the intermediate vertexes of σ; on the right side, T_0 is replaced by T'_0 (by removing the external photon in the root layer) and is connected to the begin of σ. This equivalence relation splits the terms into equivalence classes. If a term belongs to the expression, all equivalent terms also belong to the expression; it is important here that these transformations do not change the 1-particle irreducibility of the whole graph as well as of the subgraphs to which the operators are applied[28]; the absence of odd lepton loops in the whole graph is also preserved. In the sum of contributions belonging to one equivalence class, the multipliers of the form $U'_j \Gamma + U'_j \Sigma$ (as mentioned in Sec. IV B) are factorized. If the number of these multipliers is at least 1, the contribution equals 0.

The presence of M-blocks outside the $\mathcal{S}$-branch means that there is at least one factorizable M-block

---

[28]This can be proved using three facts: (1) a Feynman graph and all its subgraphs to which the operators are applied are 1-particle irreducible if and only if each layer of the corresponding layer tree is 1-particle irreducible; (2) adding and removing $(\not{p} - m)$ vertices in internal lines does not change the 1-particle irreducibility; (3) inserting the external photon into a lepton line (or removing it) does not change the 1-particle irreducibility.

in the $\mathcal{S}$-branch. If it has factorizable children, take one of them and repeat the operation until it has no factorizable children. So there is at least one factorizable M-block that has no factorizable children. The cancellation of these terms follows from this.

Note: On the one hand, the correspondence between v and σ may cross the boundaries of the layers constituting the M-block; on the other hand, the procedure of inserting and removing the external photon is always performed in the root layer of the M-block, and the structure of Σ-chains is ignored in this layer (the main path may contain special vertices); but when we move the reference, we use the main vertex of the whole M-block.

(7) *Combine the terms with different placements of the A-nodes.* After the previous step, the contribution can be written as a sum of terms like

$$(-1)^{n-1}(O_1'\Gamma_1)(O_2'\Gamma_2)...(O_n'\Gamma_n), \qquad (16)$$

where $\Gamma_1, ..., \Gamma_n$ are the vertexlike Feynman amplitudes (after the appropriate application of $-M'$ and $-U_0'$ for subgraphs) corresponding to the $\mathcal{S}$-branch elements $Y_1', ..., Y_n'$, the corresponding linear operators are $O_1', ..., O_n'$.

The Feynman graph G for which the expression is constructed is uniquely determined from the layers $Y_1', ..., Y_n'$ by a sequential insertion of the layers into a point; if $Y_1', ..., Y_{j-1}'$ have their external photons on their main paths, then Y_j' is inserted into the vertex joining the external photon; otherwise, it is inserted into the end of the main path.

The term (16) corresponding to $Y_1', ..., Y_n'$, $O_1', ..., O_n'$ exists in the expression for $\mathcal{K}$ if the following conditions are satisfied:

(i) Y_j' are correct vertexlike M-blocks (taking into account their internal layer structure);

(ii) $G \in \mathcal{K}$, where G is reconstructed by the procedure described above;

(iii) the vector $(O_1', ..., O_n')$ is of the form $(A', U_1', ..., U_1')$ or $(L' - U_1', L', ..., L', A', U_1', ..., U_1')$, where $x, ..., x$ may have 0 elements;

(iv) for all i such that $O_i' \neq A'$ the layer Y_i' has its external photon on its main path.

Any permutation of $Y_1', ..., Y_n'$ does not change the validity of $G \in \mathcal{K}$ for the reconstructed graph G.[29] Thus, the sum can be represented as a sum of terms (16) with the same conditions, but with vectors

$(O_1', ..., O_n')$ of the form $(A', U_1', ..., U_1')$ or $(A', L', ..., L', L' - U_1', U_1', ..., U_1')$.

We can prove by induction that

$$\begin{aligned}
&(U_1', U_1', U_1', ..., U_1', U_1') \\
&\quad + (L - U_1', U_1', U_1', ..., U_1', U_1') \\
&\quad + (L', L' - U_1', U_1', ..., U_1', U_1') + ... \\
&\quad + (L', L', L', ..., L', L' - U_1') \\
&= (L', L', L', ..., L', L').
\end{aligned}$$

Thus, we arrive at the sum of terms,

$$(-1)^{n-1}(A'\Gamma_1)(L'\Gamma_2)...(L'\Gamma_n), \qquad (17)$$

with the same conditions.

With the contribution of $\mathcal{K}$ obtained by the in-place on shell renormalization,[30] we perform the same operations, but without the last step and using the identities for L' and B'. These operations result in the same sum of terms (17) with the same conditions.

V. COMPUTATIONAL RESULTS

The new method was tested by numerical calculations. The contributions of 25 gauge-invariant classes contributing to $A_1^{(6)}$, $A_2^{(6)}$, $A_3^{(6)}$ for the muon were presented in [70]. Here, we present all 4-loop results for the electron and the muon for all gauge-invariant classes (with electron, muon, and tau-lepton loops). They are summarized in Table II. We used the values,

$$m_\mu/m_e = 206.76828103, \qquad m_\tau/m_\mu = 16.81665.$$

in our calculations. The uncertainty of the masses was not taken into account. The aim of the calculation was to verify the method, not to obtain precise physical results (the mass uncertainty does not play a significant role at this level of precision). Some of the previously known values for comparison that are given in the tables were calculated with other values of the mass ratios (and the uncertainties may be inaccurate). The Monte Carlo integration was performed on the ITP/TTP KIT computing cluster with the help of the GPU NVidia A100 and took about three GPU-weeks; a method similar to that described in [32,35] was used.[31]

Table III presents the computed contributions of the gauge-invariant classes from Fig. 12 to $A_1^{(8)}$ and a comparison with S. Laporta's results [29]. Table IV contains all the contributions of the classes from Fig. 13 for different

---

[29]To prove this, consider two cases: (1) each Y_j' has its external photon on its main path (in this case, the inability to jump over the external photon should be taken into account); (2) at least one Y_j' has its external photon on a lepton loop (in this case, the external photon is on a lepton loop).

[30]Note that the definition of the contribution of the gauge-invariant class in [8] already corresponds our final representation; however, it looks like it becomes cumbersome if graphs may have lepton loops.

[31]The direct usage of the methods from [32,35] is not possible for Feynman graphs having lepton loops. A modification was made; it will be explained in the further papers.

TABLE II.   The calculated total 4-loop contributions (for the electron and the muon) and their comparison with previously known values; the values for comparison are from the first reference in the lists.

Contribution	Our value	Value for comparison	Reference
$A_1^{(8)}$	$-1.9118(41)$	-1.91224576	[29]; [28,30,31]
$A_2^{(8)}(m_e/m_\mu)$	$0.000924(11)$	$0.0009141970703(372)$	[54]; [33]
$A_2^{(8)}(m_e/m_\tau)$	$0.00000710(60)$	$0.00000742924(118)$	[54]; [33]
$A_3^{(8)}(m_e/m_\mu, m_e/m_\tau)$	$0.000000745(24)$	$0.00000074687(28)$	[54]; [33]
$A_2^{(8)}(m_\mu/m_e)$	$132.673(84)$	$132.6852(60)$	[52]; [53]
$A_2^{(8)}(m_\mu/m_\tau)$	$0.04252(11)$	$0.0424941(53)$	[54]; [52]
$A_3^{(8)}(m_\mu/m_e, m_\mu/m_\tau)$	$0.0622(33)$	$0.062722(10)$	[53]; [52]

TABLE III.   Computed contributions of the classes from Fig. 12 to $A_1^{(8)}$ and their comparison with the results of [29].

| Class	Value	Value from [29]	Class	Value	Value from [29]
I(a)	$0.00087614(64)$	0.0008768659	III(7)	$-0.012485(63)$	$\cdots$
I(b)	$0.0153300(39)$	0.0153252829	IV(a)	$0.598864(69)$	0.598842072
I(c)	$0.0111324(13)$	0.0111309140	IV(b)	$0.82236(20)$	0.8222844858
I(d)	$0.049544(60)$	0.0495132026	IV(c)	$-1.13789(52)$	-1.1388228765
II(a1)	$-0.255082(24)$	$\cdots$	IV(d1)	$-0.87251(21)$	-0.872657392
II(a2)	$-0.317402(29)$	$\cdots$	IV(d2)	$-0.117978(94)$	-0.1179498688
II(a3)	$0.151986(16)$	0.1519895997	V(1)	$-1.9723(12)$	-1.9710756168
II(b1)	$-0.0341771(30)$	-0.034179376	V(2)	$-0.6227(20)$	-0.6219210635
II(b2)	$0.0065025(10)$	0.0065041484	V(3)	$-0.1412(21)$	-0.1424873798
II(c1)	$-0.0376103(54)$	$\cdots$	V(4)	$1.0865(15)$	1.0866983948
II(c2)	$-0.0536815(84)$	$\cdots$	V(5)	$-1.0397(19)$	-1.04054241
II(c3)	$0.0178533(40)$	0.0178536865	V(6)	$0.51153(71)$	0.512462048
III(1)	$0.128258(83)$	$\cdots$	II(a1) + II(a2)	$-0.572485(38)$	-0.5724718621
III(2)	$0.242948(42)$	$\cdots$	II(c1) + II(c2)	$-0.091292(10)$	-0.09130584
III(3)	$-0.04388(10)$	$\cdots$	III(1) + III(5)	$0.69078(12)$	0.6904483476
III(4)	$0.374317(49)$	0.3743579348	III(2) + III(6)	$0.409178(76)$	0.4092170285
III(5)	$0.562521(92)$	$\cdots$	III(3) + III(7)	$-0.05637(12)$	-0.0563360902
III(6)	$0.166229(64)$	$\cdots$			
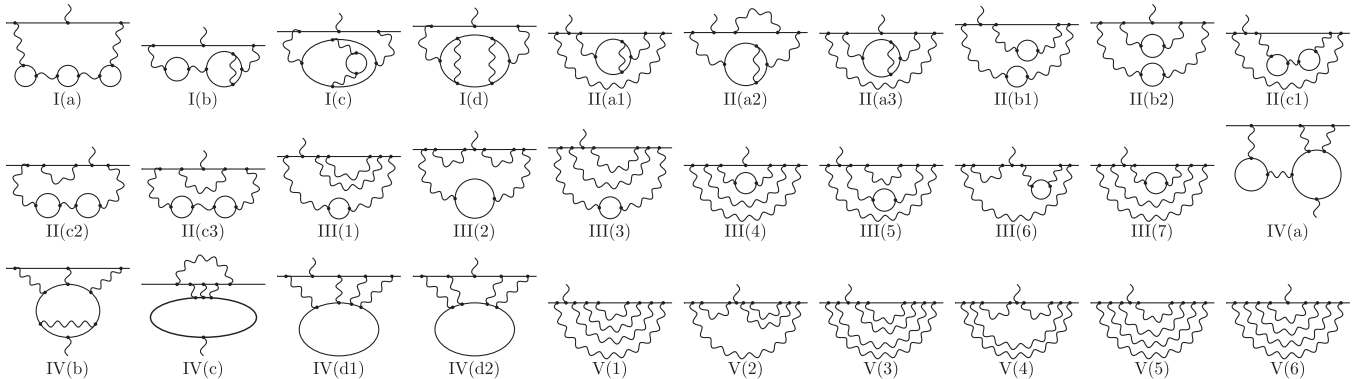
FIG. 12.   Gauge-invariant classes contributing to $A_1^{(8)}$. Each class is obtained from the corresponding picture by moving the internal photon ends along the lepton paths and loops, but without jumping over the external photon.

TABLE IV.   Calculated contributions of the classes from Fig. 13 to $A_2^{(8)}$ for electron and muon.

Class	Value $\times 10^3$, $x = e$, $y = \mu$	Value $\times 10^5$, $x = e$, $y = \tau$	Value, $x = \mu$, $y = e$	Value, $x = \mu$, $y = \tau$
I(a,xxy)	0.000168(35)	0.00003(37)	0.01854(19)	0.00002116(31)
I(a,xyx)	0.000077(18)	0.00008(22)	0.009378(80)	0.00001057(16)
I(a,yxy)	0.0000009(22)	−0.000004(13)	0.16473(32)	0.000000274(38)
I(a,yyx)	0.0000034(45)	0.000012(27)	0.32986(60)	0.000000612(77)
I(a,yyy)	0.000000006(22)	0.0000000035(78)	7.2235(18)	0.0000000180(35)
I(b,xy)	0.000963(51)	0.00050(78)	0.1195(10)	0.00014580(54)
I(b,yx)	0.000811(79)	0.0010(11)	0.33397(53)	0.00010541(69)
I(b,yy)	0.00000038(20)	0.000000053(79)	7.1267(62)	0.000001950(32)
I(c,xy)	0.004754(57)	0.00346(41)	0.16205(25)	0.00027729(30)
I(c,yx)	0.005936(32)	0.00361(37)	0.02156(40)	0.00040798(35)
I(c,yy)	0.0003543(26)	0.000127(10)	1.4372(25)	0.000053149(67)
I(d)	0.002457(32)	0.000915(62)	−0.234(15)	0.0003681(11)
II(a1)	−0.041120(60)	−0.02104(22)	−2.3873(57)	−0.0037194(13)
II(a2)	−0.07041(11)	−0.04147(57)	−2.4684(73)	−0.0054854(21)
II(a3)	0.025403(57)	0.01748(23)	2.0651(80)	0.0018698(11)
II(b1,xy)	−0.017667(63)	−0.01333(56)	−0.37697(57)	−0.00098634(55)
II(b1,yx)	−0.027301(55)	−0.02399(68)	−0.31493(55)	−0.00126397(53)
II(b1,yy)	−0.00090489(12)	−0.000319911(44)	−6.2229(30)	−0.000136912(20)
II(b2,xy)	0.006692(24)	0.00684(22)	0.16083(31)	0.00033086(24)
II(b2,yy)	0.000133460(43)	0.000047178(15)	2.1911(19)	0.0000204864(67)
II(c1,xy)	−0.04082(29)	−0.0306(33)	−0.6564(10)	−0.0022605(23)
II(c1,yy)	−0.0009045(88)	−0.000336(36)	−6.0791(24)	−0.00014068(19)
II(c2,xy)	−0.04159(30)	−0.0373(30)	−0.4278(10)	−0.0019306(26)
II(c2,yx)	−0.04159(30)	−0.0373(30)	−0.4278(10)	−0.0019306(26)
II(c2,yy)	−0.002274(22)	−0.000921(84)	−6.7191(37)	−0.00027518(40)
II(c3,xy)	0.03193(20)	0.0337(19)	0.36033(65)	0.0011914(16)
II(c3,yy)	0.0010686(85)	0.000539(36)	4.6173(27)	0.00009622(17)
III(1)	−0.0384(11)	−0.0679(70)	1.7884(74)	0.000526(12)
III(2)	0.23468(44)	0.2280(34)	1.7049(78)	0.0098734(51)
III(3)	0.0860(23)	0.073(10)	−2.703(14)	0.003569(14)
III(4)	0.2010(17)	0.1436(61)	4.375(14)	0.0111379(75)
III(5)	0.2768(11)	0.2027(75)	4.400(10)	0.016024(11)
III(6)	0.05621(29)	0.0395(15)	2.565(10)	0.0035162(48)
III(7)	0.00390(33)	−0.0013(16)	−1.3382(82)	0.0005628(56)
IV(a,xy)	0.1540(17)	0.054(16)	2.6961(53)	0.012611(17)
IV(a,yx)	0.4639(13)	0.364(13)	4.3409(74)	0.023262(12)
IV(a,yy)	0.01755(10)	0.00658(34)	116.802(27)	0.0026298(27)
IV(b)	0.04174(90)	0.0118(30)	−0.423(52)	0.006132(20)
IV(c)	−0.1954(50)	−0.114(25)	2.860(47)	−0.018337(83)
IV(d1)	−0.1693(70)	−0.092(38)	−3.5037(79)	−0.015203(55)
IV(d2)	−0.0051(45)	−0.000(28)	−0.9187(49)	−0.000555(22)

particles x and y. Since the contribution does not depend on the line directions, all graphs on the images are undirected. Also, permutting the elements on a photon does not change the contribution, but we calculated these contributions separately, except $A_2^{(8)}[\text{II}(c2, xy)]$, $A_2^{(8)}[\text{II}(c2, yx)]$ and $A_3^{(8)}[\text{II}(c2, yt)]$, $A_3^{(8)}[\text{II}(c2, ty)]$. Tables V and VI contain a comparison with known values for $A_2^{(8)}[\text{electron}]$ and $A_2^{(8)}[\text{muon}]$, respectively. Table VII contains the contributions of the classes from Fig. 14 to $A_3^{(8)}$ for electron and muon; Table VIII contains their comparison with known results.

Throughout the calculations, the operators

$$(U_j\Gamma)_\mu(p, q) = a(-m^2)\gamma_\mu,$$
$$(U_j\Sigma)(p) = s(-m^2)(\not{p} - m) + r(m^2) + s(m^2)m,$$

are used for $j = 1, 2, 3$ and all leptons, where (8) and (13) are satisfied; therefore, U-subtractions are performed at spacelike momenta ($p^2 < 0$). This is a general observation: the subtractions at spacelike points make the oscillations slightly smaller and the convergence of the Monte Carlo integration slightly faster [71].
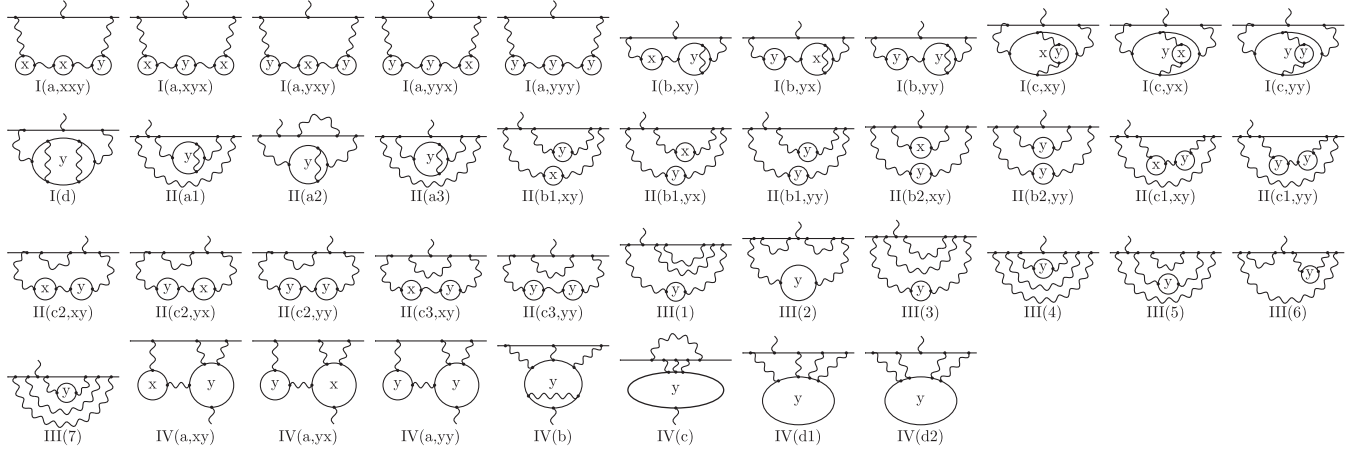
FIG. 13. Gauge-invariant classes contributing to $A_2^{(8)}$ for particle x. Each class is obtained from the corresponding image by moving the internal photon ends along the lepton paths and loops, but without jumping over the external photon. x and y may be arbitrary leptons.

For photon self-energy subgraphs, the replacement,

$$\Pi_{\mu\nu}(p^2) \to p^2 g_{\mu\nu}[h_2(0) - h_2(p^2)],$$

where (11) is implied, was used instead of subtractions. It makes the integrand simpler and its evaluation faster.

This approach was used earlier in many calculations; see, for example, [72]. Known lower-order analytical expressions for the polarization operator were not used; the reason is the attempt to make everything simple for realization. In addition, the usage of known analytical formulas can improve the calculation speed only for those contributions

TABLE V. Comparison with previously known values for $A_2^{(8)}$ of the electron ($x = e$); the values for comparison are from the first reference in the lists.

Class	Value $\times 10^3$, $y = \mu$	Value for comparison	Value $\times 10^5$, $y = \tau$	Value for comparison	Reference
I(a)	0.000250(40)	0.0002264	0.00012(43)	0.0000802	[54]; [33,55,60,61]
I(b)	0.001774(94)	0.001704139(76)	0.0015(14)	0.000602805(26)	[33]; [55]
I(c)	0.011044(66)	0.0110072(15)	0.00720(55)	0.0069819(12)	[33]
I(d)	0.002457(32)	0.0024727	0.000915(62)	0.0008746	[54]; [33]
II(a)	−0.08613(14)	−0.0864460(90)	−0.04503(65)	−0.0456480(70)	[33]; [55]
II(b)	−0.039048(87)	−0.0390003(27)	−0.03075(90)	−0.0303937(42)	[33]
II(c)	−0.09418(55)	−0.095097(24)	−0.0721(57)	−0.071697(25)	[33]
III	0.8203(33)	0.81715	0.617(16)	0.6059	[54]; [33]
IV(a)	0.6354(21)	0.63579	0.425(21)	0.451	[54]; [33]
IV(b)	0.04174(90)	0.041574	0.0118(30)	0.01471	[54]; [33,58,59]
IV(c)	−0.1954(50)	−0.19548262120(20)	−0.114(25)	−0.0979	[54]; [33]
IV(d)	−0.1744(83)	−0.1778(12)	−0.092(47)	−0.0927(13)	[33]
I(a,yyy)	0.000000006(22)	0.000000001033	0.0000000035(78)	0.000000000001293	[60]; [55,61]
$I(a, yxy)$ + $I(a, yyx)$	0.0000043(51)	0.0000001346	0.000008(30)	0.0000000003954	[60]; [55,61]
$I(a, xxy)$ + $I(a, xyx)$	0.000246(40)	0.0002263	0.00011(43)	0.00008025	[60]; [55,61]
I(b,xy)	0.000963(51)	0.0010008	0.00050(78)	0.000354	[55]
I(b,yx)	0.000811(79)	0.00070428	0.0010(11)	0.000249	[55]
I(b,yy)	0.00000038(20)	0.00000017906	0.000000053(79)	0.000000000354	[55]
$II(c1, yy)$ + $II(c2, yy)$ + $II(c3, yy)$	−0.002110(25)	−0.0021216	−0.00072(10)	−0.00075	[55]
$II(c1, xy)$ + $II(c2, xy)$ + $II(c2, yx)$ + $II(c3, xy)$	−0.09207(55)	−0.092981	−0.0714(57)	−0.0710	[55]

TABLE VI. Comparison with previously known values for $A_2^{(8)}$ of the muon ($x = \mu$); the values for the comparison are from the first reference in the lists.

Class	Value, $y = e$	Value for comparison	Reference	Value, $y = \tau$	Value for comparison	Reference
I(a)	7.7460(19)	7.745136	[53]; [52]	0.00003263(36)	0.00003242810(20)	[54]; [52]
I(b)	7.5802(63)	7.58201(71)	[52]	0.00025316(87)	0.000252	[52]
I(c)	1.6208(25)	1.624307(40)	[52]	0.00073843(47)	0.000737	[52]
I(d)	−0.234(15)	−0.2303620(50)	[56]; [52,53]	0.0003681(11)	0.0003677960(40)	[54]; [52]
II(a)	−2.791(12)	−2.77885	[53]; [52,55]	−0.0073350(26)	−0.0073290(10)	[52]
II(b)	−4.5628(37)	−4.55277(30)	[52]	−0.00203588(80)	−0.002036	[52]
II(c)	−9.3325(55)	−9.34180(83)	[52]	−0.0052501(46)	−0.0052460(10)	[52]
III	10.792(28)	10.7934(27)	[52]; [53]	0.045209(24)	0.0452089860(60)	[54]; [52]
IV(a)	123.839(29)	123.78551(44)	[52]; [53]	0.038504(20)	0.038519670(30)	[54]; [52]
IV(b)	−0.423(52)	−0.4170(37)	[52]; [53]	0.006132(20)	0.006126610(50)	[54]; [52,58,59]
IV(c)	2.860(47)	2.9072(44)	[52]; [53]	−0.018337(83)	−0.01830100(10)	[54]; [52]
IV(d)	−4.4225(93)	−4.43243(58)	[52]; [53]	−0.015757(59)	−0.015868(37)	[52]
I(a,yyy)	7.2235(18)	7.22307640(80)	[55]; [53,57]	0.000000037(14)	0.0000000232	[60]; [61]
I(b,xy)	0.1195(10)	0.1196024600(20)	[55]	· · ·	· · ·	· · ·
I(b,yx)	0.33397(53)	0.333664680(10)	[55]	· · ·	· · ·	· · ·
I(b,yy)	7.1267(62)	7.12800840(20)	[55]	· · ·	· · ·	· · ·
I(c,xy)	0.16205(25)	0.161982(11)	[74]	· · ·	· · ·	· · ·
I(c,yx)	0.02156(40)	0.0215830(20)	[74]	· · ·	· · ·	· · ·
I(c,yy)	1.4372(25)	1.440744(16)	[74]	· · ·	· · ·	· · ·
IV(a,xy)	2.6961(53)	2.69(14)	[53]	· · ·	· · ·	· · ·
IV(a,yx)	4.3409(74)	4.33(17)	[53]	· · ·	· · ·	· · ·
IV(a,yy)	116.802(27)	116.760(20)	[53]	· · ·	· · ·	· · ·
$I(a, yxy)$ $+ I(a, yyx)$	0.49459(68)	0.494072030(30)	[55]; [53,57]	0.000000885(86)	0.0000008757	[60]; [61]
$I(a, xxy)$ $+ I(a, xyx)$	0.02792(20)	0.0279883220(70)	[55]; [53,57]	0.00003173(35)	0.0000315291	[60]; [61]
$II(c1, yy)$ $+ II(c2, yy)$ $+ II(c3, yy)$	−8.1808(51)	−8.1895	[55]	· · ·	· · ·	· · ·
$II(c1, xy)$ $+ II(c2, xy)$ $+ II(c2, yx)$ $+ II(c3, xy)$	−1.1517(18)	−1.1532	[55]	· · ·	· · ·	· · ·
$II(b1, yy)$ $+ II(b2, yy)$ $+ II(c1, yy)$ $+ II(c2, yy)$ $+ II(c3, yy)$	−12.2126(63)	−12.212631	[53]	· · ·	· · ·	· · ·
$II(b1, xy)$ $+ II(b1, yx)$ $+ II(b2, xy)$ $+ II(c1, xy)$ $+ II(c2, xy)$ $+ II(c2, yx)$ $+ II(c3, xy)$	−1.6828(20)	−1.683165(13)	[53]	· · ·	· · ·	· · ·

that already require not too large numbers of the Monte Carlo samples to reach the needed accuracy; this would not affect the whole calculation speed significantly. Moreover, if the number of self-energy subgraphs is small, the "direct" realization does not lead to a significant increase in the complexity; this significantly affects only the number of the integration variables (which is not a problem for the Monte Carlo integration, provided that a good probability density function has been chosen).

VI. CONCLUSION AND DISCUSSION

The development of techniques plays a very important role in theoretical physics. Techniques of a certain kind first

TABLE VII. Computed contributions of classes from Fig. 14 to $A_3^{(8)}$ for electron and muon.

Class	Value $\times 10^7$, $x = e$	Value, $x = \mu$	Class	Value $\times 10^7$, $x = e$	Value, $x = \mu$
I(a,tty)	−0.000003(17)	−0.0000012(85)	I(c,yt)	0.0797(60)	0.000383(24)
I(a,tyt)	0.0000063(85)	0.0000038(35)	II(b1,ty)	−0.30252(13)	−0.006434(89)
I(a,xyt)	−0.0113(95)	0.000155(34)	II(b1,yt)	−0.22691(14)	−0.00457(10)
I(a,ytx)	−0.0033(93)	0.000133(30)	II(b2,yt)	0.070470(61)	0.002062(38)
I(a,yty)	0.000037(36)	0.000884(51)	II(c1,yt)	−0.533(33)	−0.00972(23)
I(a,yxt)	0.008(11)	0.000147(30)	II(c2,yt)	−0.718(63)	−0.00753(20)
I(a,yyt)	−0.000022(71)	0.00184(11)	II(c2,ty)	−0.718(63)	−0.00753(20)
I(b,ty)	0.00025(20)	0.00069(13)	II(c3,yt)	0.771(29)	0.00498(12)
I(b,yt)	0.00001(14)	0.001944(81)	IV(a,ty)	5.94(16)	0.0482(12)
I(c,ty)	0.0965(52)	0.001389(36)	IV(a,yt)	2.99(15)	0.0351(20)

appear; then they are refined: they become simpler, less cumbersome, more efficient, and only after that can the technique be extended to broader classes of tasks and lead to a breakthrough.

This work is a part of the "refinement" phase. At present, the described method of divergence subtraction works only for the lepton magnetic moments and QED. However, its formulation is much simpler and compact than that of the previously known methods. Unlike the old method described in [69], the new method has more freedom and does not require useless extra subtractions; but most importantly, the ideas behind the new method appear extendable to broader classes of problems.

It was supposed that the old method [69] only worked for $A_1^{(n)}$. However, it turned out to be suitable for the computation of $A_2^{(8)}$, $A_3^{(8)}$ as well. This was first discovered numerically and was surprising, but this can be proved: all the extra subtraction terms that the old method has have the operator L' or $L' - U'$ applied to a layer with external photon on a lepton loop. Thus, all these occurrences are canceled, as it was proved in Sec. IV C for U_3'.

The old method can also lead to the situation where subtracting a fictitious IR divergence produces a real IR divergence (see the Discussion in [69]). The cancellation of these divergences was conjectured in [69]. We have now
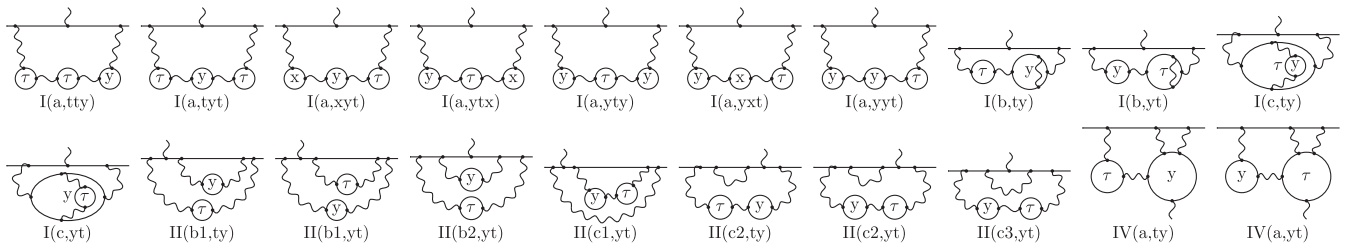

FIG. 14. Gauge-invariant classes contributing to $A_3^{(8)}$ for particle x. Each class is obtained from the corresponding image by moving the internal photon ends along the lepton paths and loops, but without jumping over the external photon. x and y are electron and muon (or vice versa), τ is the tau-lepton.

TABLE VIII. Comparison with previously known values for $A_3^{(8)}$ for the electron and the muon; the comparison values are from the first reference in the lists.

Class	Value $\times 10^7$, $x = e$	Value for comparison	Reference	Value, $x = \mu$	Value for comparison	Reference
I(a)	−0.007(17)	0.0000119956	[54]; [33]	0.00316(14)	0.003209050(10)	[53]; [52]
I(b)	0.00025(24)	0.0000140970(10)	[33]	0.00264(16)	0.002611	[52]
I(c)	0.1763(79)	0.172860(21)	[33]	0.001772(43)	0.001807	[52]
II(b)	−0.45897(20)	−0.458968(17)	[33]	−0.00895(14)	−0.0090080(10)	[52]
II(c)	−1.20(10)	−1.18969(67)	[33]	−0.01980(38)	−0.0196420(20)	[52]
IV(a)	8.93(22)	8.9432(25)	[54]; [33]	0.0834(23)	0.083747570(90)	[53]; [52]
$I(a, yty) + I(a, yyt)$	$\cdots$	$\cdots$	$\cdots$	0.00273(12)	0.00274860(90)	[57]

checked this numerically: for the only 5-loop graph in which this situation occurs, the obtained integral is indeed finite. In addition, the reasoning in Sec. IV C looks cumbersome and might contain mistakes; therefore, we checked on a computer that the required combinatorial identities are satisfied, up to six loops and three particles. However, the fact of divergence cancellation in every single Feynman graph requires a full rigorous proof.

ACKNOWLEDGMENTS

[1] F. J. Dyson, The S matrix in quantum electrodynamics, Phys. Rev. **75,** 1736 (1949).

[2] A. Salam, Divergent integrals in renormalizable field theories, Phys. Rev. **84,** 426 (1951).

[3] N. N. Bogoliubov and O. S. Parasiuk, On the multiplication of the causal function in the quantum theory of fields, Acta Math. **97,** 227 (1957).

[4] K. Hepp, Proof of the Bogolyubov-Parasiuk theorem on renormalization, Commun. Math. Phys. **2,** 301 (1966).

[5] W. Zimmermann, Convergence of Bogoliubov's method of renormalization in momentum space, Commun. Math. Phys. **15,** 208 (1969).

[6] O. I. Zavialov and B. M. Stepanov, Yad. Fys. **1,** 922 (1965), in Russian.

[7] G. S. Adkins, R. N. Fell, and J. Sapirstein, Two loop renormalization of Feynman gauge QED, Phys. Rev. D **63,** 125009 (2001).

[8] P. Cvitanović, Asymptotic estimates and gauge invariance, Nucl. Phys. **B127,** 176 (1977).

[9] A. G. Grozin, Introduction to effective field theories. 3. Bloch-Nordsieck effective theory, HQET, arXiv:1305.4245.

[10] X. Fan, T. G. Myers, B. A. D. Sukra, and G. Gabrielse, Measurement of the electron magnetic moment, Phys. Rev. Lett. **130,** 071801 (2023).

[11] J. Schwinger, On Quantum electrodynamics and the magnetic moment of the electron, Phys. Rev. **73,** 416 (1948).

[12] J. Schwinger, Quantum electrodynamics. III: The electromagnetic properties of the electron: Radiative corrections to scattering, Phys. Rev. **76,** 790 (1949).

[13] R. Karplus and N. Kroll, Fourth-order corrections in quantum electrodynamics and the magnetic moment of the electron, Phys. Rev. **77,** 536 (1950).

[14] A. Petermann, Fourth order magnetic moment of the electron, Helv. Phys. Acta **30,** 407 (1957).

[15] C. Sommerfield, Magnetic dipole moment of the electron, Phys. Rev. **107,** 328 (1957).

[16] R. Carroll and Y. Yao, α^3 contributions to the anomalous magnetic moment of an electron in the mass-operator formalism, Phys. Lett. **48B,** 125 (1974).

[17] R. Carroll, Mass-operator calculation of the electron g factor, Phys. Rev. D **12,** 2344 (1975).

[18] M. J. Levine and J. Wright, Anomalous magnetic moment of the electron, Phys. Rev. D **8,** 3171 (1973).

[19] P. Cvitanović and T. Kinoshita, Sixth order magnetic moment of the electron, Phys. Rev. D **10,** 4007 (1974).

[20] S. Laporta and E. Remiddi, The analytical value of the electron $(g-2)$ at order α^3 in QED, Phys. Lett. B **379,** 283 (1996).

[21] J. A. Mignaco and E. Remiddi, Fourth-order vacuum polarization contribution to the sixth-order electron magnetic moment, Nuovo Cimento A **60,** 519 (1969).

[22] D. Billi, M. Caffo, and E. Remiddi, A contribution to the sixth-order electron and muon anomalies, Lett. Nuovo Cimento **4,** 657 (1972).

[23] J. L. L. DeRaad, K. A. Milton, and W. Tsai, Sixth-order electron g factor: Mass-operator approach. II, Phys. Rev. D **9,** 1814 (1974).

[24] M. J. Levine, R. C. Perisho, and R. Roskies, Analytic contributions to the G factor of the electron, Phys. Rev. D **13,** 997 (1976).

[25] R. Barbieri, M. Caffo, E. Remiddi, S. Turrini, and D. Oury, The anomalous magnetic moment of the electron in QED: Some more sixth order contributions in the dispersive approach, Nucl. Phys. **B144,** 329 (1978).

[26] S. Laporta, Analytical value of some sixth order graphs to the electron $(g-2)$ in QED, Phys. Rev. D **47,** 4793 (1993).

[27] T. Kinoshita and W. B. Lindquist, Eighth-order anomalous magnetic moment of the electron, Phys. Rev. Lett. **47,** 1573 (1981).

[28] T. Aoyama, M. Hayakawa, T. Kinoshita, and M. Nio, Tenth-order electron anomalous magnetic moment—contribution of diagrams without closed lepton loops (Erratum: Phys. Rev. D **96,** 019901 (2017)); Phys. Rev. D **91,** 033006 (2015).

[29] S. Laporta, High-precision calculation of the 4-loop contribution to the electron $g-2$ in QED, Phys. Lett. B **772,** 232 (2017).

[30] P. Marquard, A. V. Smirnov, V. A. Smirnov, M. Steinhauser, and D. Wellmann, $(g-2)_\mu$ at four loops in QED, EPJ Web Conf. **218,** 01004 (2019).

[31] F. Rappl, Feynman diagram sampling for quantum field theories on the QPACE 2 supercomputer, Ph.D. thesis, Fakultät für Physik der Universität Regensburg, 2016.

[32] S. Volkov, Numerical calculation of high-order QED contributions to the electron anomalous magnetic moment, Phys. Rev. D **98,** 076018 (2018).

[33] T. Aoyama, M. Hayakawa, T. Kinoshita, and M. Nio, Tenth-order QED contribution to the electron $g-2$ and an improved value of the fine structure constant, Phys. Rev. Lett. **109,** 111807 (2012).

[34] T. Aoyama, T. Kinoshita, and M. Nio, Theory of the anomalous magnetic moment of the electron, Atoms **7,** 28 (2019).

[35] S. Volkov, New method of computing the contributions of graphs without lepton loops to the electron anomalous magnetic moment in QED, Phys. Rev. D **96,** 096018 (2017).

[36] R. Kitano and H. Takaura, QED on the lattice and numerical perturbative computation of $g-2$, Prog. Theor. Exp. Phys. **2023,** 103B02 (2023).

[37] R. Bouchendira, P. Cladé, S. Guellati-Khélifa, F. Nez, and F. Biraben, New determination of the fine structure constant and test of the quantum electrodynamics, Phys. Rev. Lett. **106,** 080801 (2011).

[38] R. H. Parker and C. Yu and W. Zhong and B. Estey and H. Müller, Measurement of the fine-structure constant as a test of the standard model, Science **360,** 191 (2018).

[39] L. Morel, Z. Yao, P. Cladé, and S. Guellati-Khélifa, Determination of the fine-structure constant with an accuracy of 81 parts per trillion, Nature (London) **588,** 61 (2020).

[40] B. Lautrup, On high order estimates in QED, Phys. Lett. **69B,** 109 (1977).

[41] M. Caffo, S. Turrini, and E. Remiddi, Higher-order radiative corrections to the electron anomaly in QED: A remark on asymptotic behaviour of vacuum polarization insertions and explicit analytic values at the first six ladder graphs, Nucl. Phys. **B141,** 302 (1978).

[42] P. A. Baikov, A. Maier, and P. Marquard, The QED vacuum polarization function at four loops and the anomalous magnetic moment at five loops, Nucl. Phys. **B877,** 647 (2013).

[43] H. H. Elend, On the anomalous magnetic moment of the muon, Phys. Lett. **20,** 682 (1966).

[44] J. Aldins, T. Kinoshita, S. J. Brodsky, and A. J. Dufner, Photon-photon scattering contribution to the sixth-order magnetic moment of the muon, Phys. Rev. Lett. **23,** 441 (1969).

[45] R. Barbieri and E. Remiddi, Electron and muon $\frac{1}{2}(g-2)$ from vacuum polarization insertions, Nucl. Phys. **B90,** 233 (1975).

[46] M. A. Samuel and G. Li, Improved analytic theory of the muon anomalous magnetic moment, Phys. Rev. D **44,** 3935 (1991).

[47] S. Laporta, The analytical contribution of the sixth-order graphs with vacuum polarization insertions to the muon $(g-2)$ in QED, Il Nuovo Cimento A **106,** 675 (1993).

[48] S. Laporta and E. Remiddi, The analytical value of the electron light-light graphs contribution to the muon $(g-2)$ in QED, Phys. Lett. B **301,** 440 (1993).

[49] M. Passera, Precise mass-dependent QED contributions to leptonic $g-2$ at order α^2 and α^3, Phys. Rev. D **75,** 013002 (2007).

[50] T. Kinoshita, B. Nizic, and Y. Okamoto, Eighth-order QED contribution to the anomalous magnetic moment of the muon, Phys. Rev. D **41,** 593 (1990).

[51] A. Czarnecki and M. Skrzypek, The muon anomalous magnetic moment in QED: Three-loop electron and tau contributions, Phys. Lett. B **449,** 354 (1999).

[52] T. Aoyama, M. Hayakawa, T. Kinoshita, and M. Nio, Complete tenth-order QED contribution to the muon $g-2$, Phys. Rev. Lett. **109,** 111808 (2012).

[53] A. Kurz, T. Liu, P. Marquard, A. V. Smirnov, V. A. Smirnov, and M. Steinhauser, Electron contribution to the muon anomalous magnetic moment at four loops, Phys. Rev. D **93,** 053017 (2016).

[54] A. Kurz, T. Liu, P. Marquard, and M. Steinhauser, Anomalous magnetic moment with heavy virtual leptons, Nucl. Phys. **B879,** 1 (2014).

[55] S. Laporta, The analytical contribution of some eighth-order graphs containing vacuum polarization insertions to the muon $(g-2)$ in QED, Phys. Lett. B **312,** 495 (1993).

[56] P. A. Baikov and D. J. Broadhurst, Three–loop QED vacuum polarization and the four–loop muon anomalous magnetic moment, arXiv:hep-ph/9504398.

[57] J.-P. Aguilar, E. de Rafael, and D. Greynat, Muon anomaly from lepton vacuum polarization and the Mellin-Barnes representation, Phys. Rev. D **77,** 093010 (2008).

[58] R. Boughezal and K. Melnikov, Hadronic light-by-light scattering contribution to the muon magnetic anomaly: Constituent quark loops and QCD effects, Phys. Lett. B **704,** 193 (2011).

[59] A. L. Kataev, Analytical eighth-order light-by-light QED contributions from leptons with heavier masses to the anomalous magnetic moment of electron, Phys. Rev. D **86,** 013010 (2012).

[60] O. Solovtsova, V. Lashkevich, and A. Sidorov, Some analytic results for the contribution to the anomalous magnetic moments of leptons due to the polarization of vacuum via lepton loops, Eur. Phys. J. Web Conf. **222,** 03007 (2019).

[61] O. P. Solovtsova, V. I. Lashkevich, and L. P. Kaptari, Lepton anomaly from QED diagrams with vacuum polarization insertions within the Mellin-Barnes representation, Eur. Phys. J. Plus **138,** 212 (2022).

[62] P. A. Baikov and K. G. Chetyrkin and J. H. Kühn and C. Sturm, The relation between the QED charge renormalized in $\overline{\text{MS}}$ and on-shell schemes at four loops, the QED on-shell β-function at five loops and asymptotic contributions to the muon anomaly at five and six loops, Nucl. Phys. **B867,** 182 (2013).

[63] A. L. Kataev, Renormalization group and the five-loop QED asymptotic contributions to the muon anomaly (Erratum: Phys. Lett. B **710,** 710 (2012)); Phys. Lett. B **284,** 401 (1992).

[64] A. L. Kataev and V. V. Starshenko, Renormalization-group-inspired approaches and estimates of the tenth-order corrections to the muon anomaly in QED, Phys. Rev. D **52,** 402 (1995).

[65] A. L. Kataev, Reconsidered estimates of the 10th order QED contributions to the muon anomaly, Phys. Rev. D **74,** 073011 (2006).

[66] S. G. Karshenboim, Tenth-order contributions to the muon anomalous magnetic moment, Yad. Fiz. **56,** 252 (1993); [Phys. At. Nucl. **56,** 857 (1993)].

[67] T. Aoyama, N. Asmussen *et al.*, The anomalous magnetic moment of the muon in the standard model, Phys. Rep. **887,** 1 (2020).

[68] L. T. Adzhemyan and M. V. Kompaniets, Five-loop numerical evaluation of critical exponents of the φ^4 theory, J. Phys. Conf. Ser. **523,** 012049 (2014).

[69] S. Volkov, Subtractive procedure for calculating the anomalous electron magnetic moment in QED and its application for numerical calculation at the three-loop level, Zh. Eksp. Teor. Fiz. **149,** 1164 (2016).

[70] S. Volkov, A method of fast calculaion of lepton magnetic moments in quantum electrodynamics, Phys. Part. Nucl. **53,** 805 (2022).

[71] S. Volkov, A flexible divergence elimination method for calculating lepton magnetic moments in quantum electrodynamics, J. Phys. Conf. Ser. **2438,** 012142 (2023).

[72] P. Cvitanović and T. Kinoshita, New approach to the separation of ultraviolet and infrared divergences of Feynman—parametric integrals, Phys. Rev. D **10,** 3991 (1974).

[73] M. E. Peskin and D. V. Schroeder, *An Introduction to Quantum Field Theory* (Perseus Books, Reading, MA, 1995).

[74] T. Kinoshita and M. Nio, Improved α^4 term of the muon anomalous magnetic moment, Phys. Rev. D **70,** 113001 (2004).